Supplemental Figure 1:
Illustrative diagrams of the kinetic reactions in the model

A, Glutamate binds to mGluRs, resulting in Gq activation.
Glu released at the synaptic cleft binds to mGluRs. Activated mGluRs in turn binds to Gq to promote the exchange of GDP to GTP of Gq. An activated Gq splits into an α subunit (Gqα) and a $\beta\gamma$ complex (G$\beta\gamma$). As far as we know, Fay *et al*. (1991) Biochemistry 30:5066-5075 is an only paper of measuring G-protein-coupled-receptor kinetics entirely, and they reported very small Gq turnover.

B, Activated PLCβ by Gq produces IP_3.
Gqα binds to PLCβ to enhance the PLCβ efficiency of IP_3 production. PLCβ has GTPase activating protein (GAP) activity, which promotes ATPase efficiency of Gq by thousands times.

C, IP_3 degradation by IP_3 3-kinase (IP3K) and IP_3 5-phosphatase (IP5P).
IP_3 degradation is extensively reviewed in a simulation study (Dunplot and Erneux (1997) Cell Calcium 22:321-331). For a review for the metabolism of inositol phosphates, see Irvine and Schell (2001) Nat Rev Mol Cell Biol 2:327-338.

D, IP_3R kinetics.
We developed a novel kinetic model of IP_3Rs based on a conceptual model in Adkins and Taylor (1999) Curr Biol 9:1115-1118. IP_3R opening requires sequential binding of IP_3 and Ca^{2+}. IP_3 binding serves to switch the Ca^{2+} sensitivity of IP_3Rs by causing inhibitory sites to be masked and a stimulatory site to be exposed.

E, Ca^{2+} release, leaks, and clearance.
We modeled Ca^{2+} release through the IP_3R Ca^{2+} channels, Ca^{2+} leaks through the plasma membrane and ER, and Ca^{2+} clearance by Ca^{2+} pumps (SERCA and PMCA) and exchangers. We assumed that molecules do not diffuse through the spine neck.

F, Ca^{2+} buffer proteins in the cytosol.
In cells, 99% of the Ca^{2+} ions are buffered with endogenous Ca^{2+}-binding proteins. In particular, cerebellar Purkinje cells contain Ca^{2+} buffers at high concentrations, and the binding ratio is more than 1000 (Fierro and Llano (1996) J Physiol 496:617-625). In addition, Ca^{2+} indicators play a role of exogenous buffers. The binding ratio dependent on $[Ca^{2+}]_i$ was extensively investigated in Maeda *et al*. (1999) Neuron 24:989-1002.

Supplemental Figure 1A

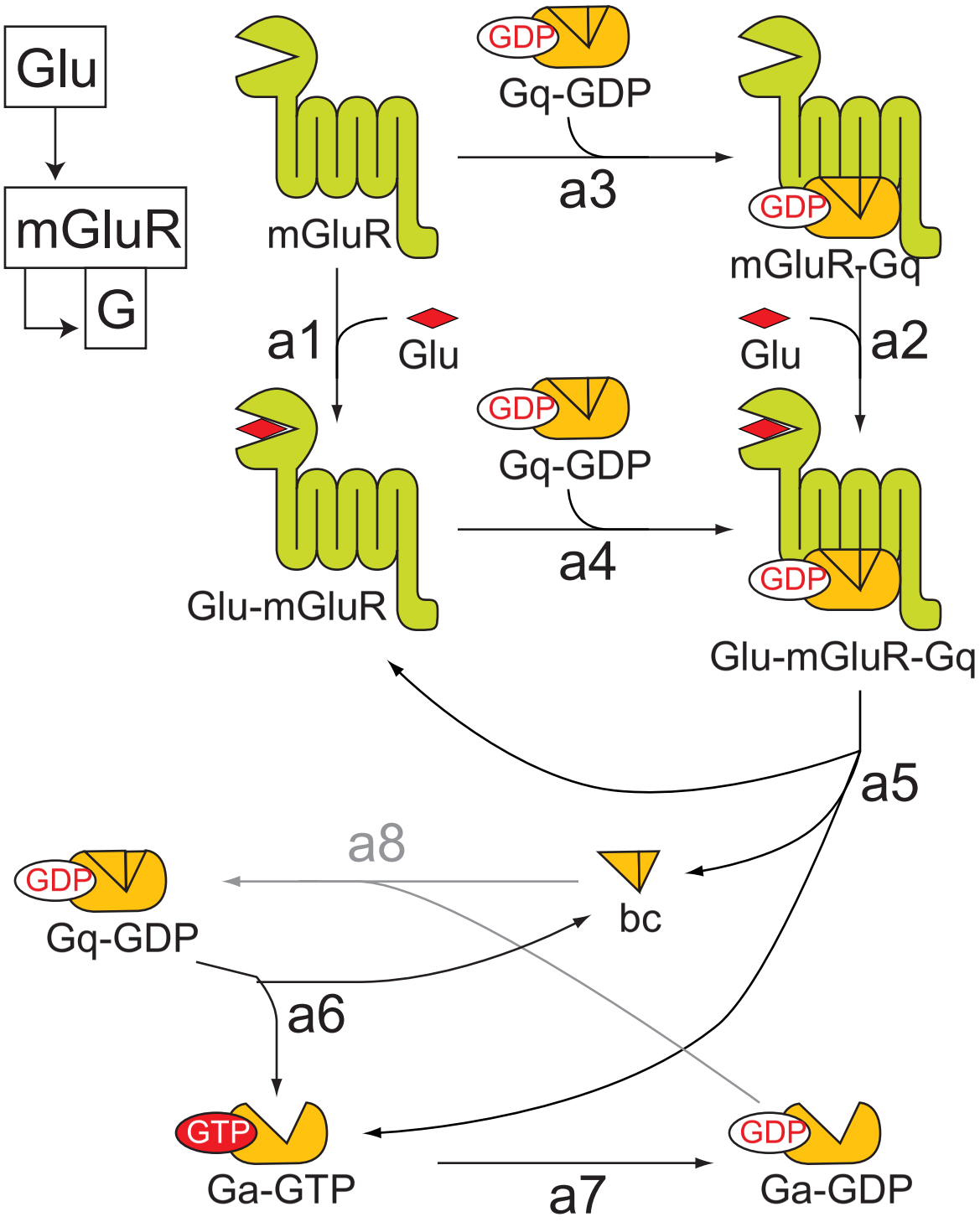

Supplemental Figure 1B

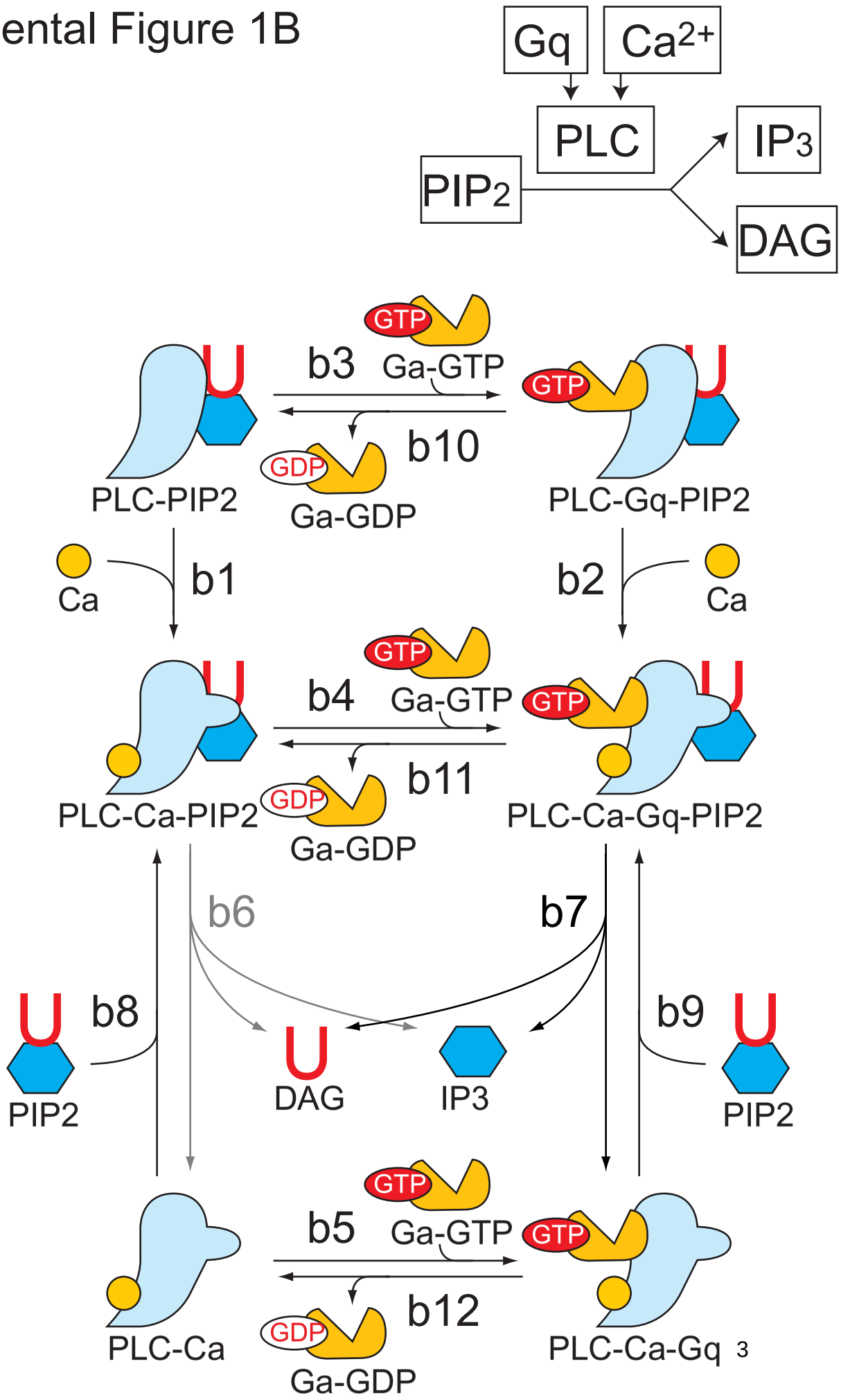

Supplemental Figure 1C

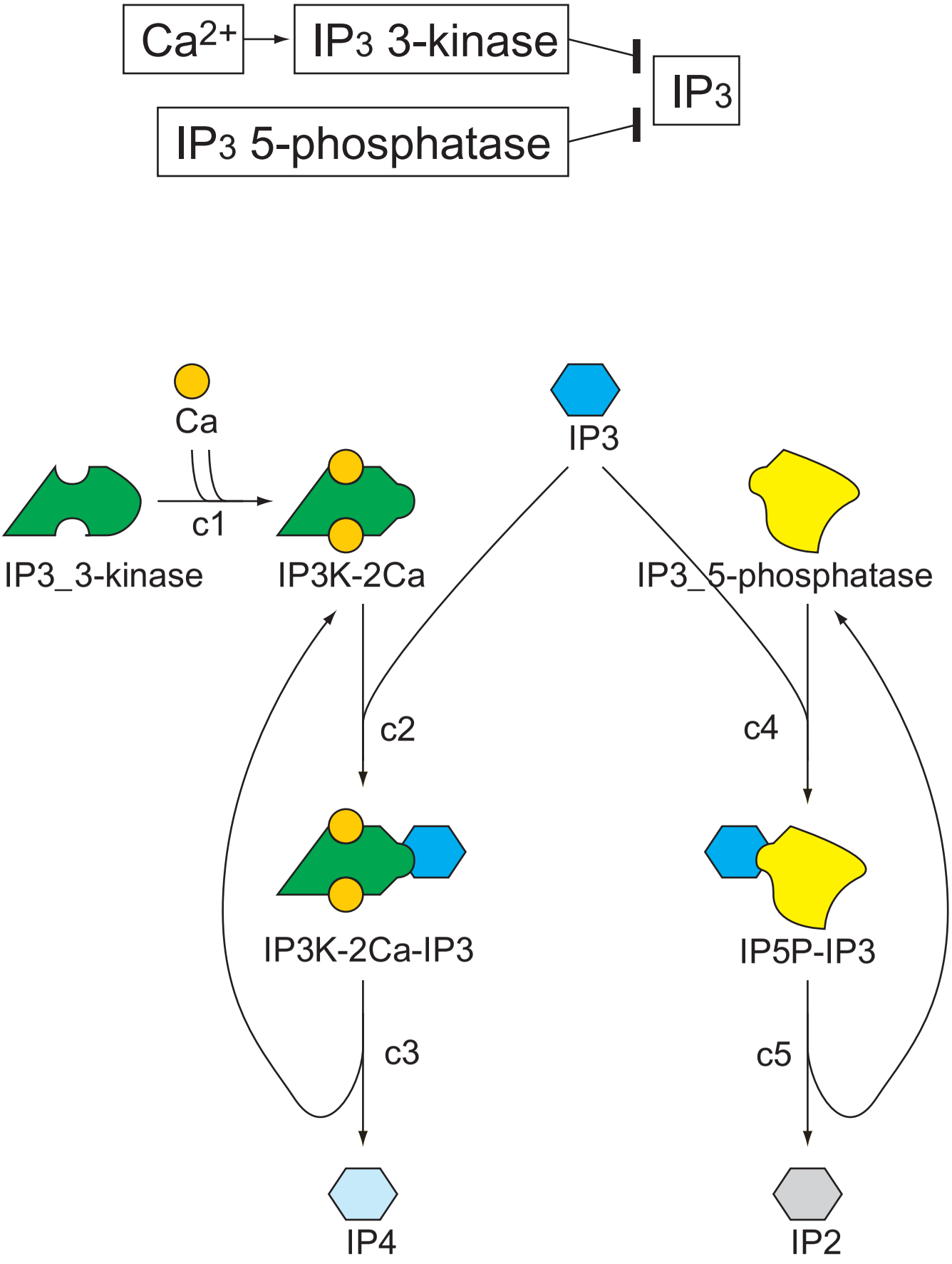

Supplemental Figure 1D

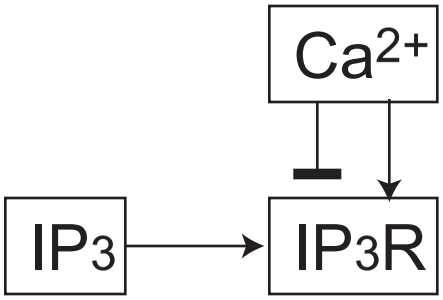

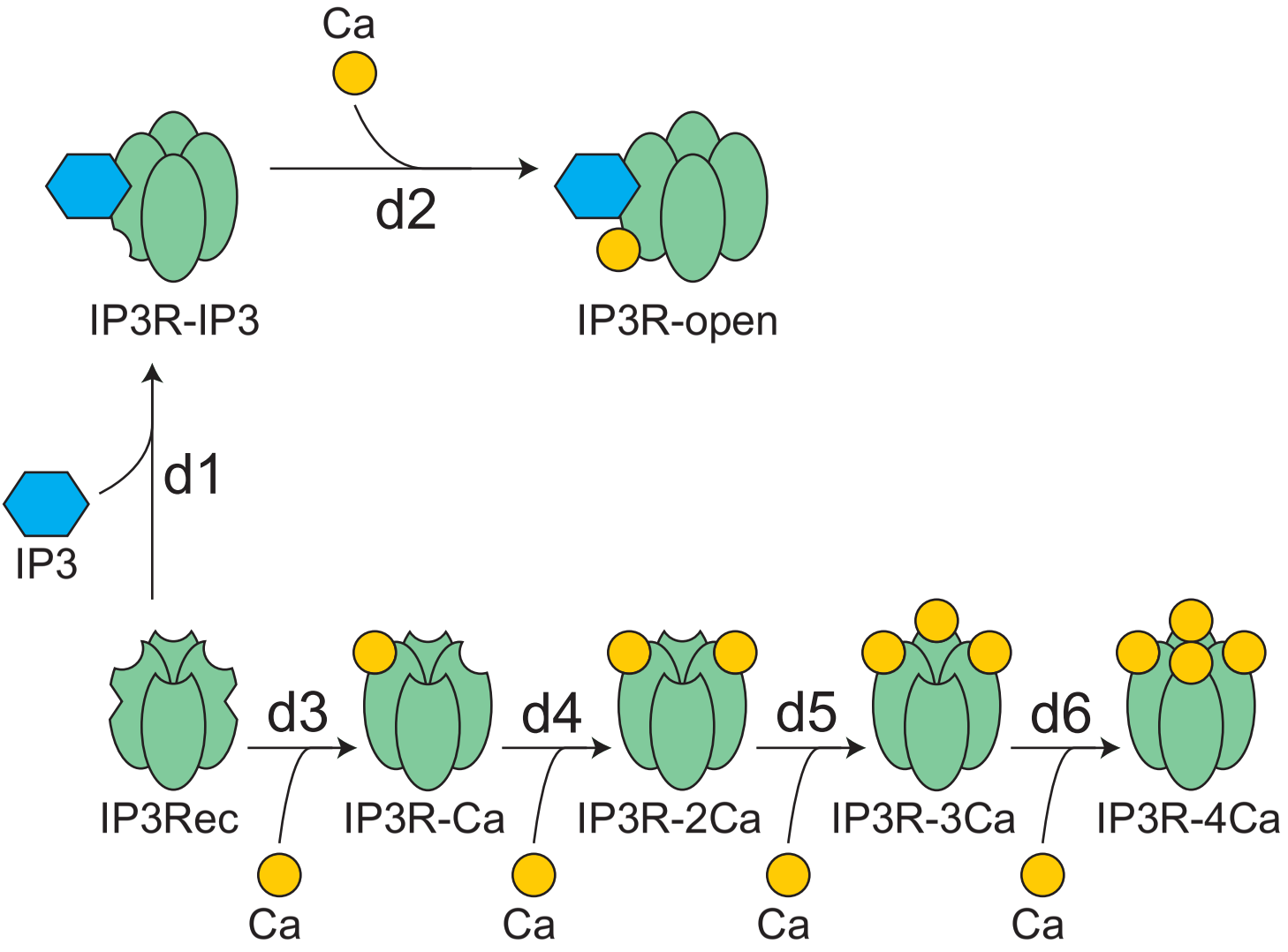

Supplemental Figure 1E

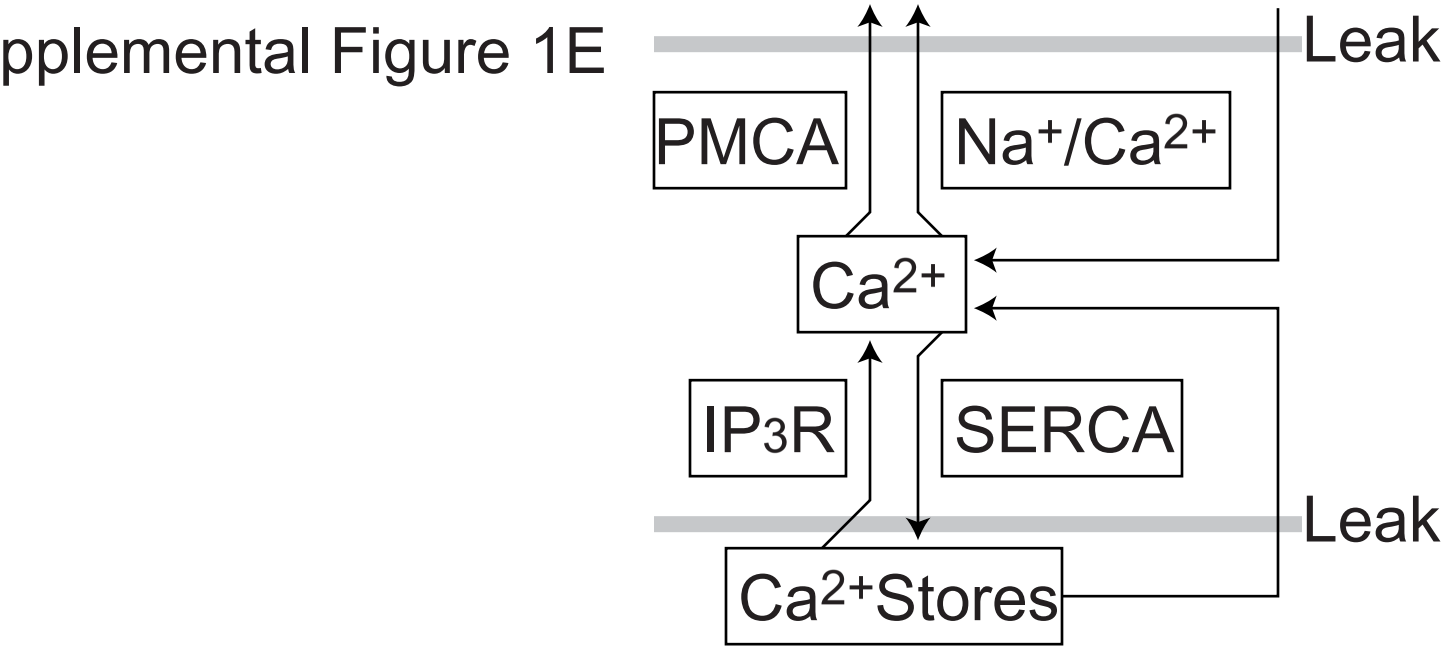

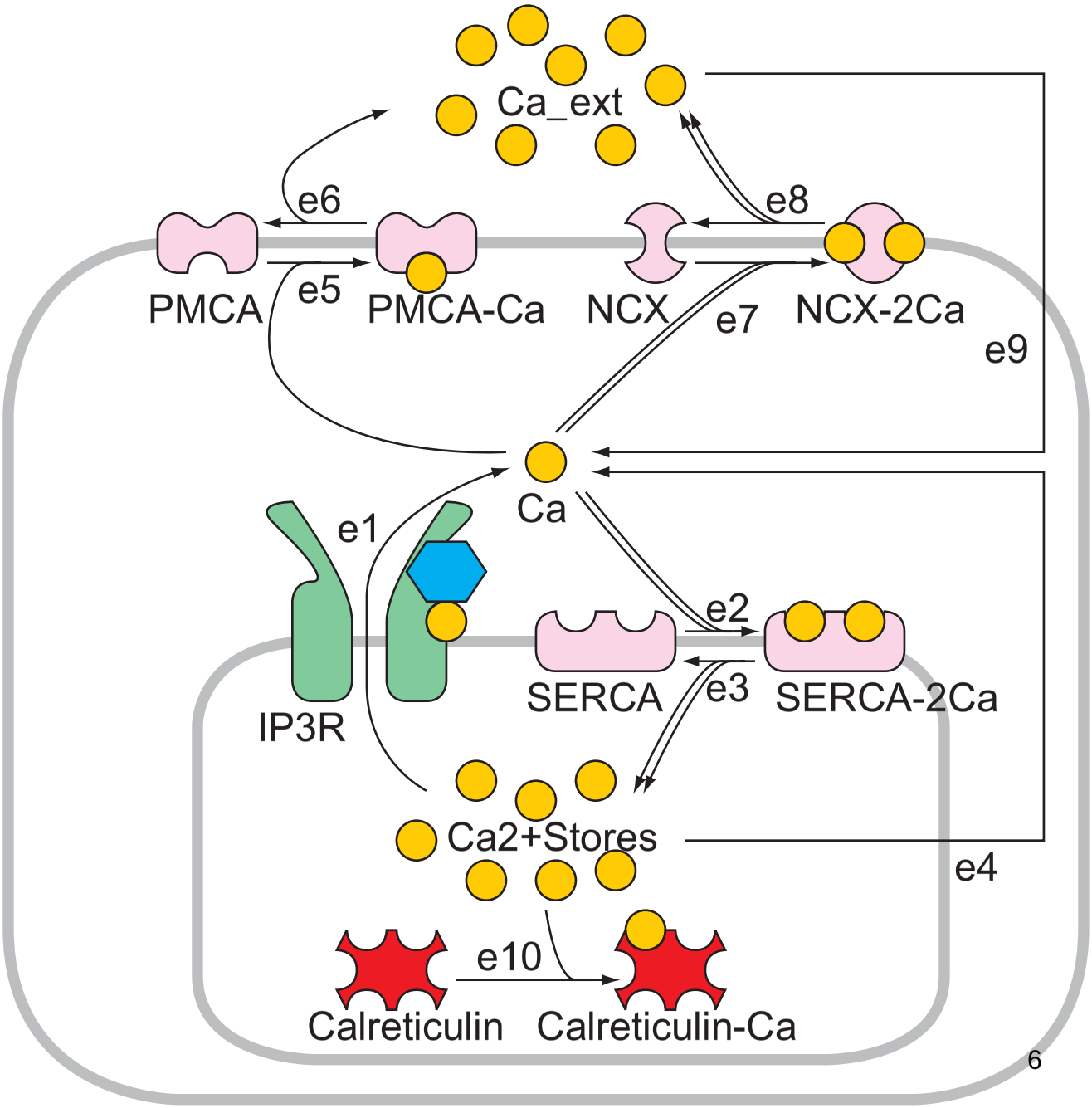

Supplemental Figure 1F

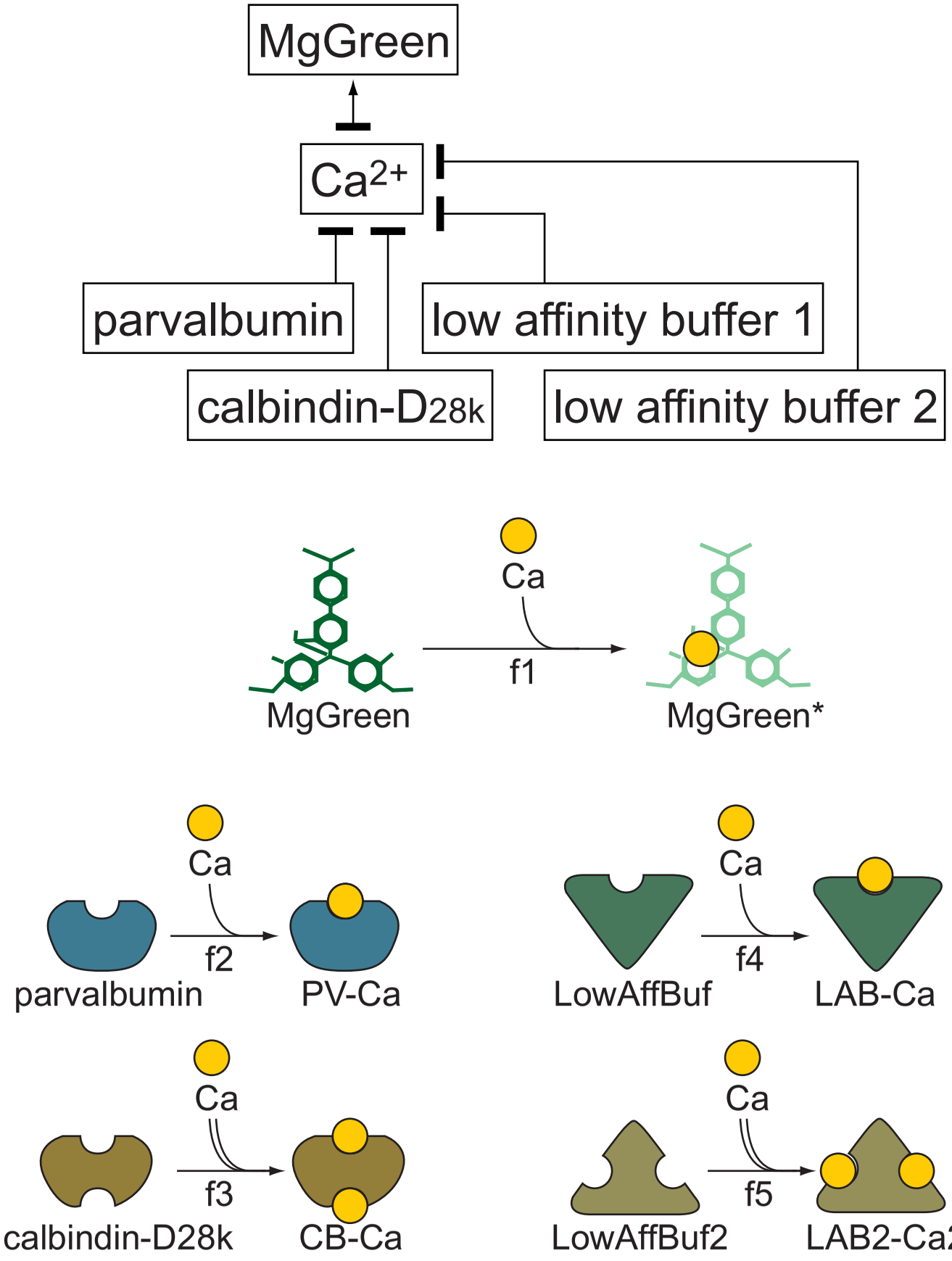

Supplemental Tables: Parameter Tables

Supplemental Table 1: Molecular numbers and concentrations in the initial condition

ID	Group	Molecular Name	#	Total #	Conc. (μM)	Total Conc.	Notes
A1	mGluR	Glu	0	300	0	250	Glutamate released at the synaptic cleft should be removed within milliseconds because individual EPSC responses can be seen with high-frequency stimuli (100 Hz), for instance, in Takechi *et al.* (1998) Nature 396:757-760. Thus, we estimated that the decaying time constant of Glu is 5 msec. The initial number of Glu that access mGluRs localized at the edge of PSD was set to 300, because concentration in neurotransmitter at the edge of spine is less than that at the center of spine (Franks *et al.* (2003) J Neurosci 23:3186-3195). This amount of Glu is sufficient to activate most of the mGluRs. # in the Supplemental Tables indicates the initial number of the molecules in its present state, and the total # indicates the total number of the molecules in any state.
A2	mGluR	mGluR	10	18	8.3333	15	Metabotropic glutamate receptor type 1. Although the characteristic of this receptor was examined in two first cloning papers (Masu *et al.* (1991) Nature 349:760-765; Houamed *et al.* (1991) Science 252:1318-1321), we cannot estimate [mGluR] because the receptors were overexpressed by functional expression in *Xenopus* oocytes. In Bhalla and Iyengar (1999) Scinece 283:381-387, they estimated 0.3 μM mGluR in a cell, and we took this value. Since the volume of the cytosol in the spine is 0.1 μm^3 in our model, the number of mGluRs was estimated to be 18. The number is similar to those of AMPARs and VGCCs in a hippocampal dendritic spine (Matsuzaki *et al.* (2001) Nat Neurosci 4:1086-1092; Sabatini and Svoboda (2000) Nature 408:589-593). We modeled that mGluRs localize at the PSD, which has 1/50-fold

ID	Group	Molecular Name	#	Total #	Conc. (μM)	Total Conc.	Notes
							volume of the cytosol. We obtained 8.3333 μM mGluR in the PSD.
A3	mGluR	mGluR-Glu	0	18	0	15	mGluRs activated by Glu binding.
A4	mGluR	Gq-GDP	52	60	43.333	50	Trimeric G-protein Gq family. In Bhalla and Iyengar (1999) Science 283:381-387, they estimated 1.0 μM Gq in a cell. Since the cytosolic volume in the spine is 0.1 μm^3, the number of Gq was estimated to be 60. We obtained 50 μM Gq in the PSD because the cytosol has 50-fold volume of the PSD.
A5	mGluR	mGluR-Gq	8	18	6.6667	15	mGluRs binding to Gq without Glu. It is not clear whether mGluRs and Gq form complex before ligand stimulation (small K_d), or ligand stimulation on mGluRs leads to the binding of mGluRs and Gq (large K_d). In this model, we assumed half of the mGluRs bind Gq before glutamate release.
A6	mGluR	Glu-mGluR-Gq	0	18	0	15	Intermediated state for Gq activation of Glu-mGluR-Gq complex.
A7	mGluR	Ga-GTP	0	60	0	50	Activated Gqα subunit. Gq-GTP binds PLCβ to enhance IP_3 productivity of PLCβ.
A8	mGluR	Gbc	0	60	0	50	G-protein βγ complex. In this simulation, there are no proteins activated by Gβγ.
A9	mGluR	Ga-GDP	0	60	0	50	Inactivated Gqα subunit. Gα-GDP rapidly binds Gβγ to form a trimer.
B1	PLC	PIP2	5000	5000	4166.7	4166.7	Phosphatidylinositol-4,5-bisphosphate. Molecular biology of the cell 4th edition says that 5000000 lipid molecules exist in a 1 μm^2 area of the plasma membrane. Since PIP_2 is a minor lipid (less than 1%), the number of PIP_2 in the PSD was estimated to be 5000.
B2	PLC	PLC-PIP2	42	50	35	41.667	PLCβ subtype 4. We modeled PLCβ to bind PIP_2 before PLC activation by Ca^{2+}, because PIP_2 concentration is high enough to bind almost all PLC in saturation. Bhalla and Iyengar (1999)

ID	Group	Molecular Name	#	Total #	Conc. (μM)	Total Conc.	Notes
							Science 283:381-387 estimated 0.8 μM PLCβ in a cell. Since the cytosolic volume in the spine is 0.1 μm^3, the number of Gq was estimated to be 50. We obtained 42 μM PLCβ in the PSD because the cytosol has 50-fold volume of the PSD.
B3	PLC	PLC-PIP2-Ca	7.5	50	6.25	41.667	Without Gq, PLCβ activity is very low.
B4	PLC	PLC-PIP2-Gq	0	50	0	41.667	This state has no enzyme activity. PLCβ4 requires Ca^{2+} for activation.
B5	PLC	PLC-PIP2-Ca-Gq	0	50	0	41.667	Fully activated form of PLCβ4. PLCβ hydrolyzes PIP_2 into DAG and IP_3. PLCβ4 activation is dependent on Gq, whereas some other PLCβ subtypes are not.
B6	PLC	PLC-Ca	0.5	50	0	41.667	The intermediate states of PLCβ that do not bind PIP_2. We assumed that PLCβ in the basal states bind PIP_2.
B7	PLC	PLC-Ca-Gq	0	50	0	41.667	
B8	PLC	DAG	0	0	0	0	Diacylglycerol activates no enzyme in the model because we do not implement DAG-dependent enzymes such as protein kinase C.
B9	PLC	IP3_PSD	0.12	12	0.1	10	IP_3 is produced by PLCβ in the PSD and diffuses to the cytosol.
C1	IP3deg	IP3_spine	6	600	0.1	10	We set the basal [IP_3] to 0.1 μM in this simulation. [IP_3] measurement in living cells is difficult. The only report is Luzzi *et al.* (1998) J Biol Chem 273:28657-28662. They estimated 0.04 μM IP_3 in *Xenopus* Oocytes by using capillary electrophoresis.
C2	IP3deg	IP3_3-kinase	52	54	0.86667	0.9	IP_3 3-kinase, which phosphorylates IP_3 to IP_4. In Takazawa *et al.* (1989) Biochem J 261:483-488, 0.020 mg of protein was purified from 700 g of bovine brain tissue. The yield was 4.4% and the molecular weight was 35000. Thus, 0.020 mg x (100%/4.4%) / (35000 g/mol) / 0.7 liter = 0.019 μM while assuming the specific gravity of the tissue 1 kg/liter. This enzyme is highly localized in Purkinje dendritic spines (Yamada *et al.* (1993) Brain Res

ID	Group	Molecular Name	#	Total #	Conc. (μM)	Total Conc.	Notes
							606:335-340; Go *et al.* (1993) Neurosci Lett 158:135-138). Therefore, we increased [IP3K] to 0.9 μM.
C3	IP3deg	IP3K-2Ca	2	54	0.033333	0.9	Ca^{2+}-bound state of IP3K.
C4	IP3deg	IP3K-2Ca-IP_3	0	54	0	0.9	Ca^{2+}- and IP_3-bound state of IP3K.
C5	IP3deg	IP3_5-phos	58.8	60	0.98	1	IP_3 5-phosphatase, which dephosphorylates IP_3 to IP_2. From Verjans *et al.* (1992) Eur J Biochem 204:1083-1087, 0.806 mg of IP5P was obtained from 2 kg of brain tissue. The yield was 15% and the molecular weight was 43,000. Thus, 0.806 mg x (100%/15%) / (43000 g/mol) / 2 liter brain = 0.06 μM, while assuming the specific gravity of the tissue 1 kg/liter. A study using antibodies showed that the enzyme was highly expressed in the Purkinje neurons (De Smedt *et al.* (1996) JBC 271:10419-10424). Thus, we increased it to 1 μM.
C6	IP3deg	IP5P-IP3	1.2	60	0.02	1	Intermediate binding state of IP_3 5-phosphatase and IP_3.
D1	IP3R	IP3Rec	14.22	16	0.237	0.26667	IP_3R type 1 is highly expressed in Purkinje cells. We counted 16 immunogold spots in the figure of the PF spine slice in Otsu *et al.* (1990) Cell Struct Function 15:163-173. Since the slice has 1/4 thickness of a spine and IP_3Rs are homotetramers, the number of IP_3Rs in a PF spine was estimated to be 16 (= 16 /(1/4) /4).
D2	IP3R	IP3R-IP3	0.06	16	0.1	0.26667	IP_3-bound state of IP_3Rs. In our IP_3R kinetics model, IP_3 binding to IP_3Rs allows activation of the IP_3Rs by Ca^{2+}.
D3	IP3R	IP3R_open	0.01	16	0.00016667	0.26667	Open state of IP_3Rs.
D4	IP3R	IP3R-Ca	1.5	16	0.025	0.26667	Inactivation state of IP_3Rs, bound to one Ca^{2+} ion.
D5	IP3R	IP3R-2Ca	0.18	16	0.003	0.26667	Inactivation state of IP_3Rs, bound to two Ca^{2+} ions.
D6	IP3R	IP3R-3Ca	0.03	16	0.0005	0.26667	Inactivation state of IP_3Rs, bound to three Ca^{2+} ions.
D7	IP3R	IP3R-4Ca	0	16	0	0.26667	Inactivation state of IP_3Rs, bound to four Ca^{2+} ions.

ID	Group	Molecular Name	#	Total #	Conc. (μM)	Total Conc.	Notes
E1	CaReg	CaSpine	3.6	3.6	0.06	0.06	Free cytosolic Ca^{2+} concentration, $[Ca^{2+}]_i$. The basal $[Ca^{2+}]_i$ is set to 0.06 μM.
E2	CaReg	Ca2+PSD	0.072	0.072	0.06	0.06	Ca^{2+} concentration in the postsynaptic density. This concentration is used only for Ca^{2+}-dependent PLCβ activation. It has a slight effect on IP_3 productivity of PLCβ in the PSD.
E3	CaReg	SERCA	148	155	2.4667	2.5833	Sacro- and endoplasmic reticulum Ca^{2+}-ATPase. SERCA is a dominant protein in the ER, constituting 80% of the ER membrane protein (Stryer Biochemistry 5th edition). SERCA type 2 is dominant in the Purkinje cells (Takei *et al.* (1992) J Neurosci 12:489-505). We assumed the number of SERCA so that $[Ca^{2+}]_{ER}$ is 150 μM at the basal state.
E4	CaReg	SERCA-2Ca	7	155	0.11667	2.5833	Ca^{2+}-bound state of SERCA.
E5	CaReg	PMCA	68	108	1.1333	1.8	Plasma membrane Ca^{2+}-ATPase. Type 2 of PMCA is abundant in Purkinje cells (de Talamoni *et al.* (1993) PNAS 90:11949-11953). PMCA has higher affinity and lower capacity than Na^+/Ca^{2+} exchangers. At the basal $[Ca^{2+}]_i$, PMCA pumps out much more Ca^{2+} ions than Na^+/Ca^{2+}. We chose [PMCA] so that $[Ca^{2+}]_i$ is 0.06 μM at the basal state.
E6	CaReg	PMCA-Ca	40	108	0.66667	1.8	Ca^{2+}-bound state of PMCA.
E7	CaReg	NCX	32	32	0.53333	0.53333	Na^+/Ca^{2+} exchangers. They use Na^+ electrochemical gradient across the plasma membrane as their energy source. Note that we do not model membrane potential. NCXs play a major role in pumping out intracellular Ca^{2+} at micromolar levels of $[Ca^{2+}]_i$,.
E8	CaReg	NCX-2Ca	0	32	0	0.53333	Ca^{2+}-bound state of Na^+/Ca^{2+} exchangers.
E9	CaReg	CaStore	1800	30000	150	2500	Free Ca^{2+} concentration in the ER, $[Ca^{2+}]_{ER}$, was previously assumed to be more than 1 mM in 1990s (for example, Fiala *et al.*

ID	Group	Molecular Name	#	Total #	Conc. (μM)	Total Conc.	Notes
							(1996) J Neurosci 16:3760-3774; Bezprozvanny and Ehrich (1994) J Gen Physiol 104:821-856). Recent studies using low-affinity Ca^{2+} indicators implied $[Ca^{2+}]_{ER}$ at submicromolar levels (e.g. Park *et al.* (2000) EMBO J 19:5729-5739). Thus, we used 150 μM $[Ca^{2+}]_{ER}$ in the simulation.
E10	CaReg	calreticulin	$9.6x10^5$	$1.032x10^6$	80000	86000	A well-known Ca^{2+} buffer in the ER. We took the Ca^{2+} biding ratio in the ER to be 5. Bound Ca^{2+} is 5 times free Ca^{2+} in the ER at the basal $[Ca^{2+}]_{ER}$.
E11	CaReg	calreticulin-Ca	72,000	$1.032x10^6$	6000	86000	Ca^{2+}-bound state of calreticulin.
E12	CaReg	Ca_ext	$1.2x10^7$	$1.2x10^7$	2000	2000	Extracellular Ca^{2+} concentration.
F1	CaBuf	MgGreen	14940	15000	249	250	Magnesium Green 1. This low-affinity Ca^{2+} indicator was used at 250-500 μM in Wang e*t al.* (2000) Nat Neurosci 3:1266-1273. To compare our simulation results with the Ca^{2+} imaging directly, we included 250 μM MgGreen in our model.
F2	CaBuf	MgGreen*	60	15000	1	250	Ca^{2+}-bound form of MgGreen. MgGreen* (Ca^{2+}-bound form) has twice the fluorescence of MgGreen (Ca^{2+}-nonbound form). Thus, $F_{max}/F_{min} = 2$.
F3	CaBuf	parvalbumin	1380	3000	23	50	Parvalbumin is highly expressed in GABAergic neurons, including Purkinje cells (de Talamoni *et al.* (1993) PNAS 90:11949-11953). Considering the high binding ratio at the basal $[Ca^{2+}]_i$ (Fierro and Llano (1996) J Physiol 496:617-625), the concentration in parvalbumin should be tens of micromolars.
F4	CaBuf	PV-Ca	1620	3000	27	50	Ca^{2+}-bound state of parvalbumin.
F5	CaBuf	Calbindin-D28k	5850	6000	97.5	100	Calbindin-D_{28k} is highly expressed in Purkinje cells. Ca^{2+} decay in mutant mice with no calbindin-D_{28k} gene was faster than in wild-type mice (Airaksinen *et al.* (1997) PNAS 94:1488-1493).

ID	Group	Molecular Name	#	Total #	Conc. (μM)	Total Conc.	Notes
							Although Maeda *et al.* (Neuron 24:989-1002 (1999)) studied the effect of Ca^{2+} buffers in cerebellar Purkinje cells and estimated 360 μM [CB], they neglected effects of other high-affinity buffers and Ca^{2+} pumps dependent on $[Ca^{2+}]_i$. [CB] was estimated to be 100 μM in our simulation.
F6	CaBuf	CB-2Ca	150	6000	2.5	100	Ca^{2+}-bound state of calbindin-D_{28k}.
F7	CaBuf	LowAffBuf	5997	6000	99.95	100	Purkinje cells contain low-affinity buffers at high concentrations (Maeda *et al.* (1999) Neuron 24:989-1002). We fitted the binding ratio in our model to the binding ratio in their Fig. 6 by using two buffers. Low-affinity buffer 1 (LAB) is non-cooperative, and Hill coefficient is 1.
F8	CaBuf	LAB-Ca	3	6000	0.05	100	Ca^{2+}-bound state of low-affinity buffer 1.
F9	CaBuf	LowAffBuf2	6000	6000	100	100	Purkinje cells contain low-affinity buffers at high concentration (Maeda *et al.* (1999) Neuron 24:989-1002). We fitted the biding ratio curve in their Fig. 6 by using two buffers. Low-affinity buffer 2 (LAB2) is cooperative, and the Hill coefficient is 2.
F10	CaBuf	LAB2-2Ca	0	6000	0	100	Ca^{2+}-bound state of low-affinity buffer 2.

Supplemental Table 2: Kinetic rate constants in the reactions

ID	Group	Reaction Name	k_f	k_b (/sec)	K_d (μM)	Notes
a1	mGluR	Glu_bind_mGluR	11.11	100	9	The dependency of slow EPSCs on glutamate concentrations was measured in the first two cloning papers (Masu *et al.* (1991) Nature 349:760-765; Houamed *et al.* (1991) Science 252:1318-1321). We took the K_d value from Masu *et al.* (1991) Nature 349:760-765.
a2	mGluR	Glu_bind_mGluR-Gq	11.11	100	9	
a3	mGluR	mGluR_bind_Gq	2	100	50	The value of K_d influences whether mGluRs can bind Gq in the resting state. Higher K_d tends to allow mGluRs to bind Gq before glutamate release, whereas lower K_d does not. We assumed that half of the mGluRs are bound to Gq at the basal state.
a4	mGluR	mGluR-Glu_bind_Gq	2	100	50	The detailed balance determines the K_d value from the loop, mGluR → Glu-mGluR → Glu-mGluR-Gq → mGluR-Gq → mGluR.
a5	mGluR	Activate_Gq	116			As far as we know, there is only one paper that measured k_{cat} for Gq activation by G-protein coupled receptors (Fay *et al.* (1991) Biochemistry 30:5066-5075). Unfortunately, they used muscarinic cholinergic receptors (mAchRs), not mGluRs, as G-protein coupled receptors. Reported k_{cat} value was 0.01 /sec, and taken in two simulation papers (Fiala *et al.* (1996) J Neurosci 16:3760-3774; Bhalla and Iyengar (1999) Science 283:381-387). This value was too small to yield micromolar IP_3 concentrations in our simulation. We neglect the reported parameter value and arbitrarily assumed k_{cat} of 116 /sec.
a6	mGluR	Basal-ActGq	0.0001			Basal activity of exchange of GDP to GTP in Gq. The reaction is so slow that it can be neglected.
a7	mGluR	Inact_Gq	0.02			From Berstein *et al.* (1992) JBC 267:8081-8088, k_{cat} for GTPase activity of Gq itself is only 0.8 /min. Gq inactivation is facilitated by PLC in this simulation.
a8	mGluR	Trimerize_Gq	6			The parameter value determines the speed of binding Gqα-GDP and Gβγ. This reaction is thought to be fast. We used the same value as in Bhalla and Iyengar (1999) Science 283:381-387. Although 6 /sec of k_f might seem to be small, trimerization completes within 1 sec after glutamate stimulation.
b1	PLC	PLC-PIP2_bind_Ca	300	100	0.3333	Ca^{2+}-dependency of PLCβ4 activity has not been quantitatively measured. We

ID	Group	Reaction Name	k_f	k_b (/sec)	K_d (μM)	Notes
						took the K_d value from the parameters in PLCβ1 (Smrcka *et al.* (1991) Science 251:804-807), as well as Bhalla and Iyengar (1999) Science 283:381-387.
b2	PLC	PLC-PIP2-Gq_bind_Ca	900	30	0.03333	Ca^{2+}-dependency of PLCβ4 activity has not been quantitatively measured. We took the K_d value from the parameters in PLCβ1 (Smrcka *et al.* (1991) Science 251:804-807), as Bhalla and Iyengar (Science 283:381-387 (1999)) did. Note that the basal $[Ca^{2+}]_i$ is enough to activate PLC-PIP2-Gq.
b3	PLC	PLC-PIP2_bind_Gq	800	40	0.05	The detailed balance determines the K_d value from the loop, PLC-PIP2 → PLC-Ca-PIP2 → PLC-Ca-Ga-PIP2 → PLC-Gq-PIP2 → PLC-PIP2.
b4	PLC	PLC-PIP2-Ca_bind_Gq	1200	6	0.005	From Fig. 4 in Lee *et al.* (1994) JBC 269:25335-25338, affinity for Gαq is 5 nM. Because of this high affinity, most of the activated Gα bind PLCβ in our simulation.
b5	PLC	PLC-Ca_bind_Gq	1200	6	0.005	
b6	PLC	IP3_prd_without_Gq	2			PLCβ4 has basal activity of IP_3 production without Gq. The measurement of this activity is difficult because PLCβ4 is inhibited by ribonucleotides (Lee *et al.* (1994) JBC 269:25335-25338). Therefore, we assumed this parameter to hold basal $[IP_3]$ at 0.1 μM.
b7	PLC	IP3_prd_with_Gq	160			The measurement of this enzyme activity is difficult because PLCβ4 is inhibited by ribonucleotides (Lee *et al.* (1994) JBC 269:25335-25338). We used the activity of PLCβ1 in Mishra and Bhalla (2002) Biophys J 83:1298-1316.
b8	PLC	PLC-Ca_bind_PIP2	1	170	170	A biochemical paper reported K_m of 100-200 μM for PIP_2 in several types of PLCβ (James *et al.* (1995) JBC 270:11872-11881). We took the affinity of PLCβ1 (K_m = 170 μM).
b9	PLC	PLC-Ca-Gq_bind_PIP2	1	170	170	
b10	PLC	inact_Gq_by_PLC-PIP2	8			PLCβ4 has GAP (G-protein activation protein) activity, which enhances the GTPase efficiency of Gq to thousands times. In the review of Montel (2000) Nat Cell Biol 2:E82-E83, the half-time of Gq inactivation is estimated to be 25-75 msec in the existence of PLC. We used the same activity among different PLCβ4 states.
b11	PLC	inact_Gq_by_PLC-PIP2-Ca	8			
b12	PLC	inact_Gq_by_PLC-Ca	8			
c1	IP3deg	IP3K_bind_2Ca	1111.1	100	0.3	We took the K_d value from a Ca^{2+} simulation paper (Dunplot and Erneux (1997)

ID	Group	Reaction Name	k_f	k_b (/sec)	K_d (μM)	Notes
						Cell Calcium 22:321-331). K_m for Ca^{2+} = 0.3 μM and Hill coefficient = 2.
c2	IP3deg	IP3K-2Ca_bind_IP3	100	80	0.8	We took the K_m value from a Ca^{2+} simulation paper (Dunplot and Erneux (1997) Cell Calcium 22:321-331). Michaelis constant K_m is 1 μM. $K_m = (k_b + k_{cat}) / k_f$ = (80 + 20) / 100 = 1 μM.
c3	IP3deg	IP3K_deg_IP3	20			Several studies reported very different V_{max} values (Irvine *et al.* (1986) Nature 320:631-634; Takazawa *et al.* (1989) Biochem J 261:483-488; Choi *et al.* (1990) Science 248:64-66). Thus, we did not take any reported value from these studies.
c4	IP3deg	IP5P_bind_IP3	9	72	8	We took the K_m value from a Ca^{2+} simulation paper (Dunplot and Erneux (1997) Cell Calcium 22:321-331). Michaelis constant K_m = 1 μM. $K_m = (k_b + k_{cat}) / k_f$ = (72 + 18) / 9 = 10 μM.
c5	IP3deg	IP5P_deg_IP3	18			A purification study reported that V_{max} = 20-35 μmol/min/mg protein (Verjans *et al.* (1992) Eur J Biochem 204:1083-1087). IP_3 5-phosphatase is a 43kDa enzyme, and we obtained k_{cat} = 20-35 x 43000/60000 = 18 #/sec/# protein. This unit conversion method was described in De Schutter (2000) Computational Neuroscience, CRC Press, Boca Raton, pp. 31.
d1	IP3R	IP3R_bind_IP3	1000	25800	25.8	From measurement of Ca^{2+} depletion of the ER stores, the affinity of IP_3Rs for IP_3 in Purkinje cells is much lower (K_d = 25.8 μM) than *in vitro* (Fujiwara *et al.* (2001) Neuroreport 12:2647-2651). The low affinity is consistent with the fact that Ca^{2+} response to IP_3 uncaging in Purkinje cells require strong photostimulus ([IP_3] > 10 μM) for (Khodakhah and Ogden (1993) PNAS 90:4976-4980; Finch and Augustine (1998) Nature 396:753-756). Thus, we used K_d of 25.8 μM in the simulation.
d2	IP3R	IP3R-IP3_bind_Ca	8000	2000	0.25	Ca^{2+} directly binds to IP_3Rs for activation. From a bell-shaped Ca^{2+}-dependency of IP_3Rs (Bezprozvanny and Ehric (1994) J Gen Physiol 104:821-856; Fujiwara *et al.* (2001) Neuroreport 12:2647-2651), we obtained K_d = 0.25 μM. The reaction must be faster than Ca^{2+}-dependent IP_3R inactivation for Ca^{2+} positive feedback.

ID	Group	Reaction Name	k_f	k_b (/sec)	K_d (μM)	Notes
d3	IP3R	IP3R_bind_Ca	8.889	5	0.56249	IP_3Rs are completely inactivated at high concentrations of $[Ca^{2+}]_i$ (< 10 μM). In our kinetic model, an IP_3R has four Ca^{2+} inactivation sites. This sequential Ca^{2+} binding reaction was assumed to be positively cooperative. In other words, Ca^{2+} ions bind a subunit easier as more Ca^{2+} binds to IP_3Rs. How to estimate these parameters is written in Ca^{2+}-dependent IP_3R inactivation in the Material and Methods.
d4	IP3R	IP3R-Ca_bind_Ca	20	10	0.5	
d5	IP3R	IP3R-2Ca_bind_Ca	40	15	0.375	
d6	IP3R	IP3R-3Ca_bind_Ca	60	20	0.33333	
e1	CaReg	IP3R_Ca_channel	450	450	(perm)	In Bezprozvanny and Ehrich (1994) J Gen Physiol 104:821-856, they estimated that 5400 Ca^{2+} ions go through an open IP_3R per second at 2500 μM $[Ca^{2+}]_{ER}$. The unit of permability is not described in GENESIS/kinetikit, but we found that the parameter value of 450 matches the estimation.
e2	CaReg	SERCA_bind_2Ca	17147	1000	0.24149	We took the kinetics parameter of SERCA subtype 2b from Lytton *et al.* (1992) JBC 267:14483-14489. K_m = 0.27 μM and the Hill coefficient = 2. $K_m^2 = (k_b + k_{cat}) / k_f = (1000 + 250) / 17147 = (0.27\ \mu M)^2$.
e3	CaReg	SERCA_uptake	250			In Stryer Biochemistry 5th edition, one SERCA pumps out less than 100 Ca^{2+} ions per second. Thus, we took k_{cat} value to be 50 /s at first, but the low k_{cat} value caused a problem. The speed of Ca^{2+} clearance does not increase in proportion to the number of Ca^{2+} pumps because free Ca^{2+} concentration becomes low and the Ca^{2+} binding to the pump decreases in the large presence of Ca^{2+} pumps with low k_{cat}. We failed to reproduce Ca^{2+} time course showed in Wang *et al.* (2000) Nat Neurosci 3:1266-1273 even if we increased the number of pumps. Following the fact that most of the other Ca^{2+} simulation neglect the binding effect of Ca^{2+} pumps, we decided to reduce the buffing effect by adjusting k_{cat} and [SERCA], while keeping V_{max} (= k_{cat} x [SERCA]). Thus, we increased k_{cat} 5-fold and decreased [SERCA] 1/5-fold.
e4	CaReg	Ca_Leak_from_ER	15	15	(perm)	This leak parameter was dependent on other parameters of Ca^{2+} regulation.
e5	CaReg	PMCA_bind_Ca	25000	2000	0.08	We took the kinetic parameters of PMCA subtype 2 from Stauffer *et al.* (1995) JBC 270:12184-12190. K_m = 0.1 μM and Hill coefficient = 1. $K_m = (k_b + k_{cat}) / k_f = (500 + 2000) / 25000 = 0.1$ μM.

ID	Group	Reaction Name	k_f	k_b (/sec)	K_d (μM)	Notes
e6	CaReg	PMCA_uptake	500			The capacity of PMCA was increased to 10 times (50 to 500) for the same reason as the increase in k_{cat} for SERCA.
e7	CaReg	NCX_bind_2Ca	93.827	4000	6.5293	Since this model does not include voltage, the efficacy of Na^+/Ca^{2+} uptake should be dependent only on Ca^{2+} concentration, not on the membrane potential. In Fujioka *et al.* (2000) J Physiol 529:611-623, they measured Ca^{2+}-dependent current of Na^+/Ca^{2+}. K_m for Ca^{2+} = 7.3 μM and the Hill coefficient = 2. $K_m^2 = (k_b + k_{cat}) / k_f = (4000 + 1000) / 93.287 = (7.3\ \mu M)^2$.
e8	CaReg	NCX_uptake	1000			Stryer Biochemistry 5th edition says that a Na^+/Ca^{2+} can extrude 2,000 Ca^{2+} ions per second. Since the Hill coefficient is 2, a Na^+/Ca^{2+} transports 2 Ca^{2+} ions at one reaction cycle. Thus, $k_{cat} = 2000/2 = 1000$ /s.
e9	CaReg	Ca_Leak_from_ext	10	10	(perm)	This leak parameter was dependent on other parameters of Ca^{2+} regulation.
e10	CaReg	Ca_bind_calreticulin	0.1	200	2000	Calreticulin is a high-concentration and uncooperative buffer. We took K_d to be 2 mM, according to Krause and Michalak (1997) Cell 88:439-443.
f1	CaBuf	Ca_bind_MgGreen	1000	19000	19	Apparent K_d of Magnesium Green 1 for Ca^{2+} is 19 μM in the presence of endogenous Mg^{2+}, from Wang *et al.* (2000) Nat Neurosci 3:1266-1273.
f2	CaBuf	PV_bind_Ca	18.5	0.95	0.05315	Parvalbumin is a slow and high-affinity buffer. Most of the parvalbumin binds endogenous Mg^{2+} at the basal Ca^{2+} concentration,. In Lee *et al.* (2000) J Physiol 525:419-431, they measured the apparent dissociation constant K_d = 0.0514 μM and the unbinding rate constant k_b = 0.95 /sec in the presence of Mg^{2+}, and we used the parameter values.
f3	CaBuf	CB_bind_2Ca	87	11.275	0.36	Calbindin is a cooperative and high-affinity buffer. We took the K_d value and the Hill coefficient to be 0.36 μM and 2, from Maeda *et al.* (1999) Neuron 24:989-1002. These values were consistent with (2:2) ratio in Table 1 in Nagerl *et al.* (2000) Biophys J 79:3009-3018.
f4	CaBuf	LAB_bind_Ca	10	1000	100	We included low-affinity buffers based on Fig. 6 in Maeda *et al.* (1999) Neuron 24:989-1002. The Hill coefficients of low-affinity buffer 1 (LAB) and low-affinity buffer 2 (LAB2) were taken 1 and 2, respectively.
f5	CaBuf	LAB2_bind_2Ca	1	4000	20	

Supplemental Table 3: Categories of parameters

	known				unknown
	Form Purkinje cells	From other cells	From reaction in test tubes	From other molecular subtypes	
Time constants, τ		f2, f3	a6, a8, e1, e4 ,e9		a1, a2, a3, a4, b1, b2, b3, b4, b5, b8, b9, c1, c2, c4, d1, d2, d3, d4, d5, d6, e2, e5, e7, e10, f1, f4, f5
Dissociation constants, K_d and Michaelis constants, K_m	d1, d2, d3, d4, d5,d6	a1, a2, a4, f1, f2, f3	b4, b5, c1, c2, c4, e2, e5, e7, e10	b1, b2, b3, b8, b9	a3, f4 ,f5
Enzyme turnovers, V_{max}		b10, b11, b12	a7, c5, e3, e6, e8	b7	a5, b6, c3
Initial concentrations, [ ]	$[Ca^{2+}]_i$, IP_3R, MgGreen, parvalbumin, calbindin-D_{28k}, low-affinity buffer, low-affinity buffer 2	Glu, mGluR, Gq, IP_3, $[Ca^{2+}]_{ER}$, $[Ca^{2+}]_{ext}$, calreticulin	PIP_2, IP_3 3-kinase, IP_3 5-phosphatase	PLCβ4 (taken from PLCβ1)	SERCA, PMCA, Na^+/Ca^{2+}

Supplemental Figure 2:
Analysis of parameter sensitivity to the IP_3 time course and time window function.

We investigated the sensitivity of our model to variations of all known and unknown parameters (total of 96 parameters). All parameter values listed in Supplemental Tables 1, 2 were given as explained in Methods and notes in the Supplemental Tables (the default parameter value set).

A-E, Parameter sensitivity to the IP_3 time course. Each value of the known and unknown parameters was varied in a range of 1/100—100 times while maintaining the values of all other parameters, and the IP_3 time course with PF-alone input was re-computed. *A*, An example of re-computed IP_3 time course. The maximum enzyme velocity for Gq activation by Glu-mGluR was varied to 2, 5, 10, 20, 50, and 100 (red and bold lines) and 1/2, 1/5, 1/10, 1/20, 1/50, and 1/100 times (pink and broken lines). *B-E*, The peak time and peak amplitude of IP_3 time course when we varied the values of time constants (*B*), dissociation and Michaelis constants (*C*), maximum enzyme velocities (*D*), and initial molecular concentrations (*E*).

F-K, Parameter sensitivity to the time window of Ca^{2+} response. Each value of the known and unknown parameters was varied in a range of 1/100—100 times while maintaining the values of all other parameters, and the time window function was re-computed as well as the IP_3 time course. *F*, An example of re-computed time window. The time constant for binding Glu and mGluR was varied to 2, 5, 10, 20, 50, and 100 (red and bold lines) and 1/2, 1/5, 1/10, 1/20, 1/50, and 1/100 times (pink and broken lines). *G*, For quantitative comparisons, we used three features: the peak time, half-width, and peak amplitude of the Gaussian function fitted to the time window. The time windows were analyzed in the time interval from -500 to 600 ms. *H-K*, The three features of time window when we varied the values of time constants (*H*), dissociation and Michaelis constants (*I*), maximum enzyme velocities (*J*), and initial molecular concentrations (*K*).

The shapes of the symbols indicate the magnitude of varying the parameter values (◯:1/2 or 2; △: 1/5 or 5; ▽: 1/10 or 10; □: 1/20 or 20; ◇: 1/50 or 50; ☆: 1/100 or 100). The colors of the symbols indicate the direction of varying the parameter value (light color: decrease; dark color: increase) and whether the parameter is known or unknown (blue: known; red: unknown). When the symbols of one parameter gather together on the dashed line (control), the IP_3 time course and time window are robust against variations of the parameter value.

Supplemental Figure 2A

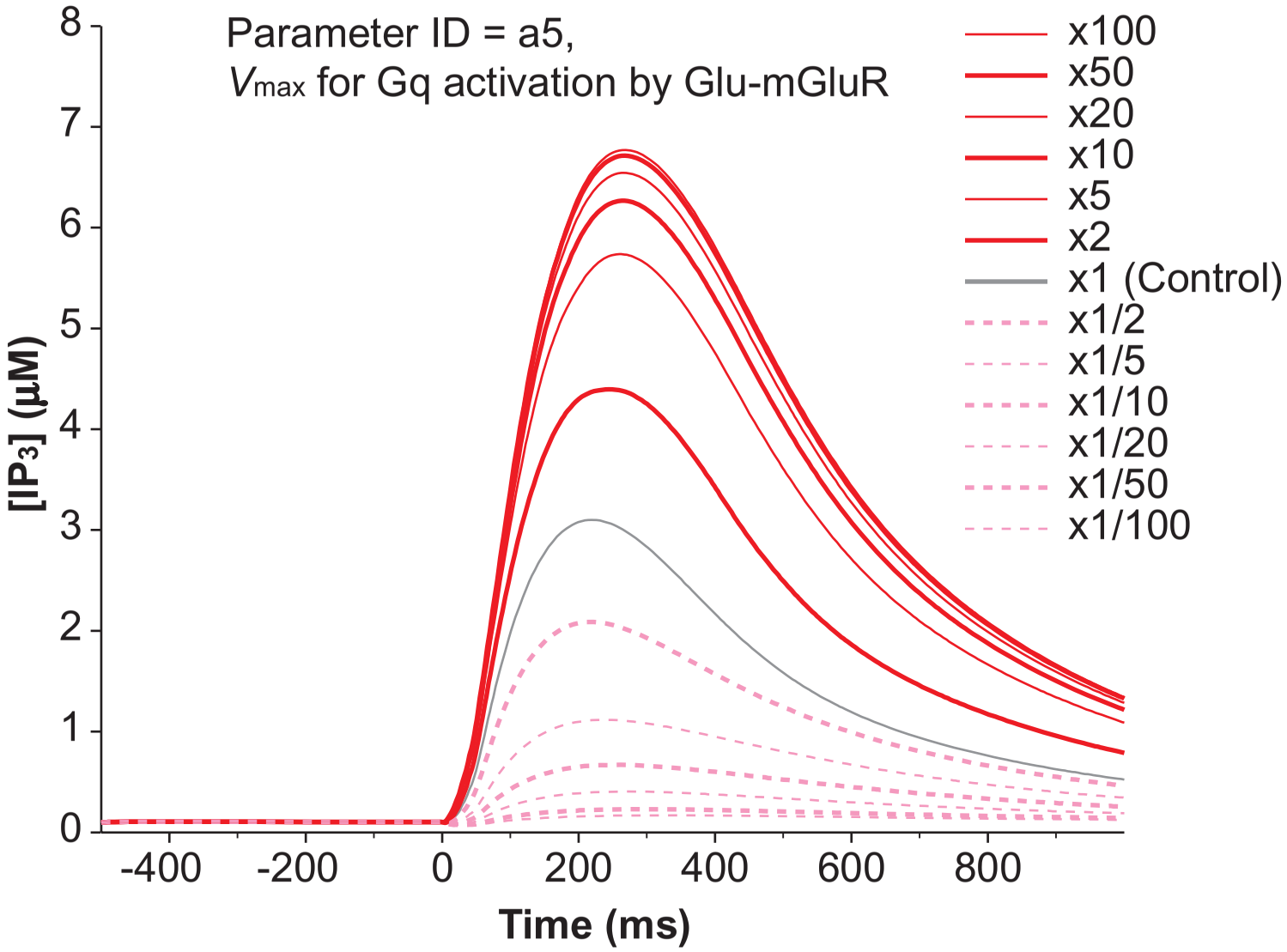

Supplemental Figure 2B

	x1/100	x1/50	x1/20	x1/10	x1/5	x1/2	x2	x5	x10	x20	x50	x100
known	☆	◇	□	▽	△	○	○	△	▽	□	◇	☆
unknown	☆	◇	□	▽	△	○	○	△	▽	□	◇	☆

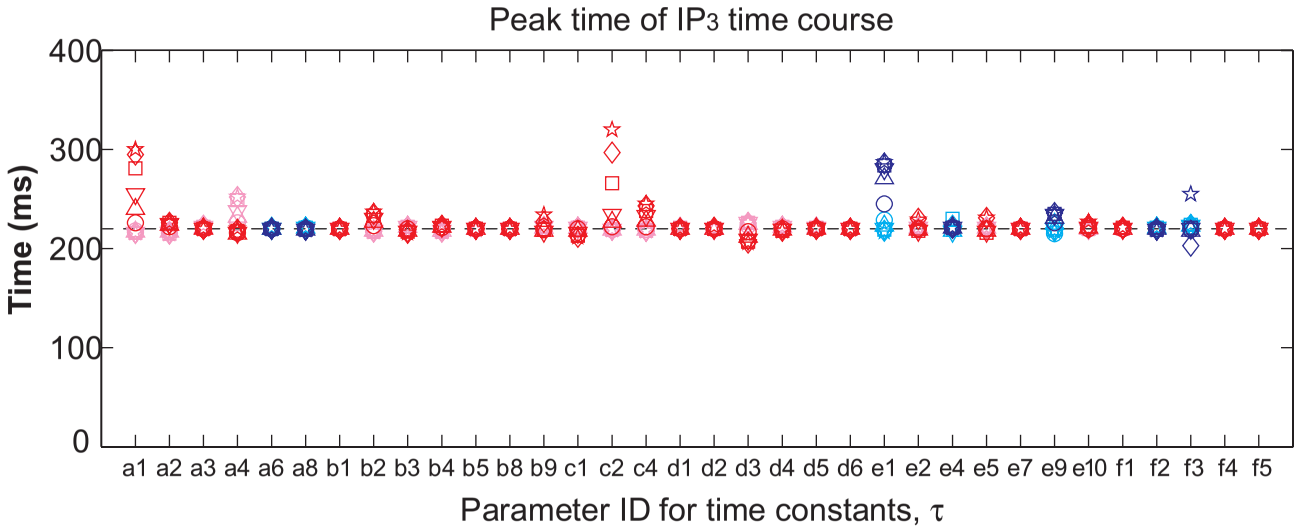

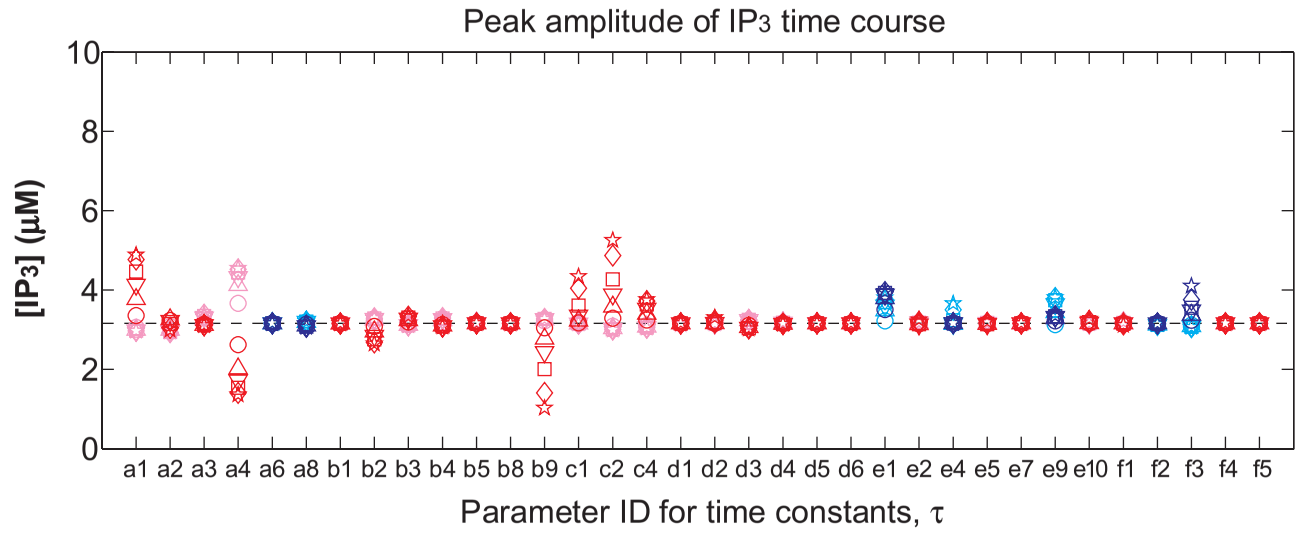

Supplemental Figure 2C

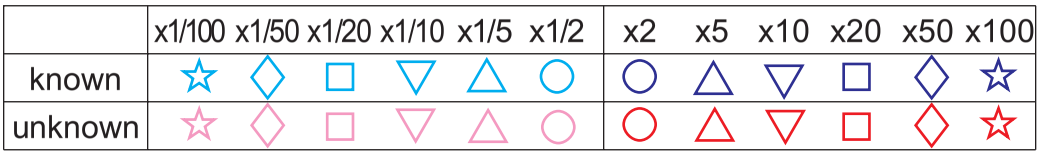

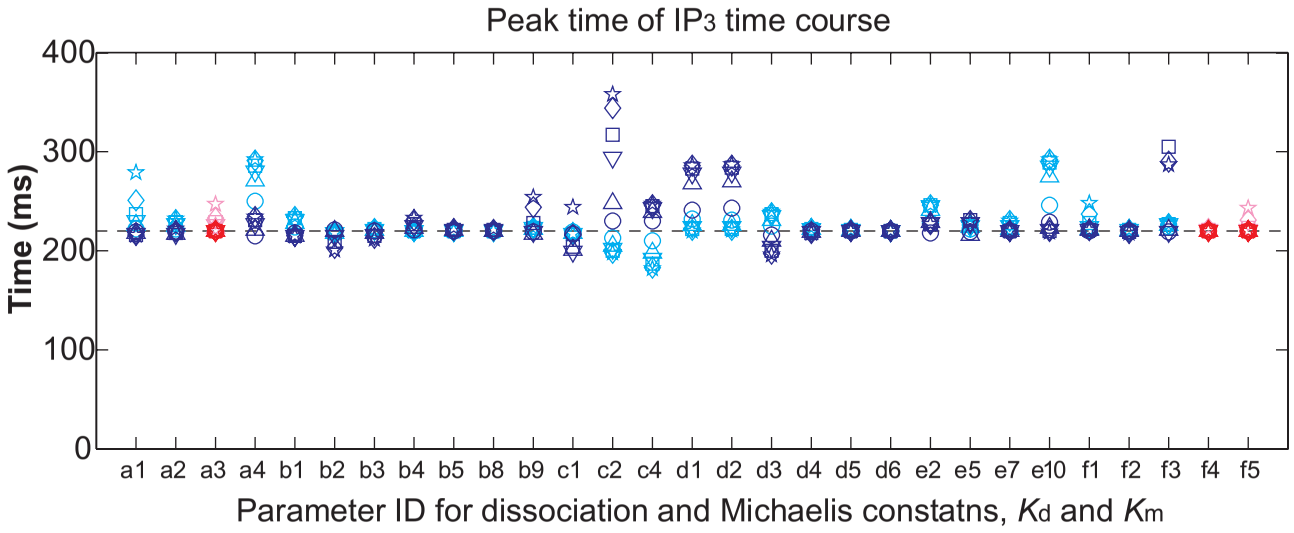

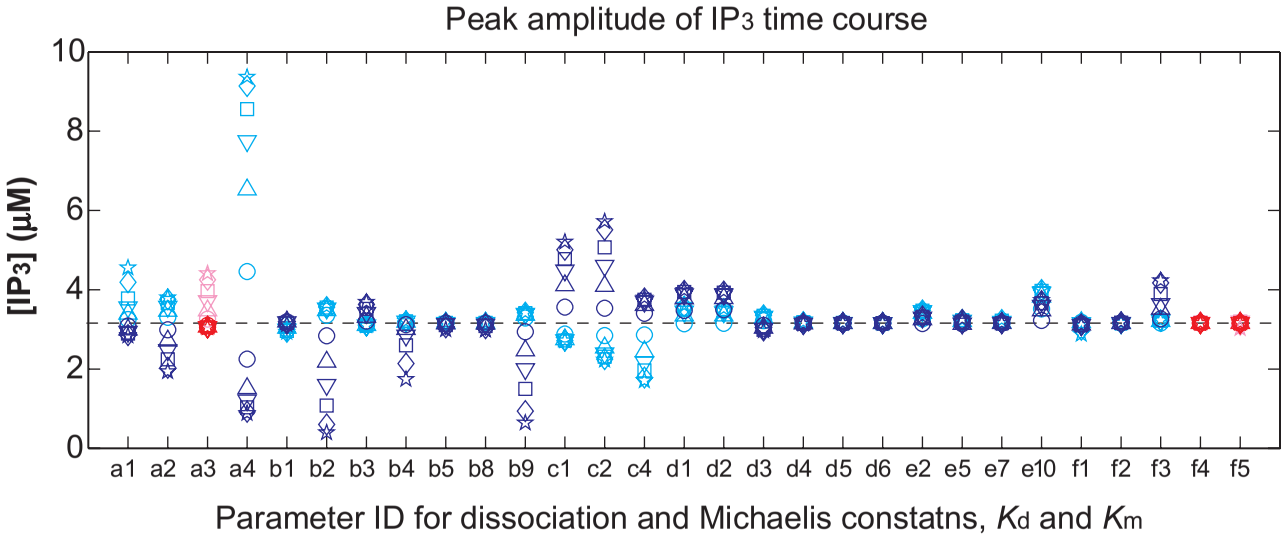

Supplemental Figure 2D

	x1/100	x1/50	x1/20	x1/10	x1/5	x1/2	x2	x5	x10	x20	x50	x100
known	☆	◇	□	▽	△	○	○	△	▽	□	◇	☆
unknown	☆	◇	□	▽	△	○	○	△	▽	□	◇	☆

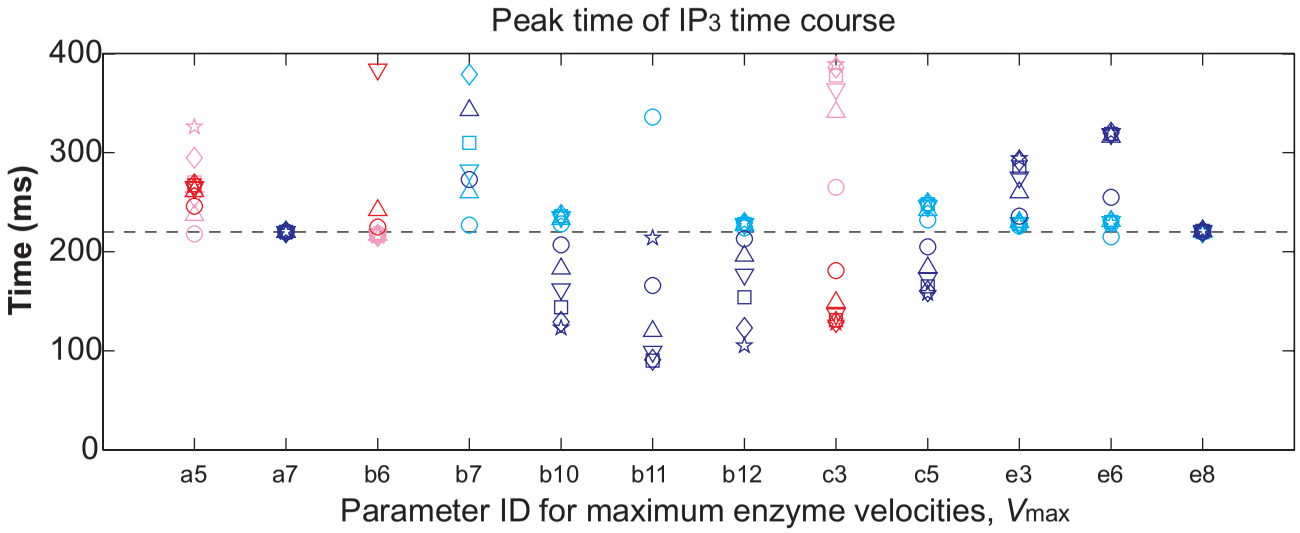

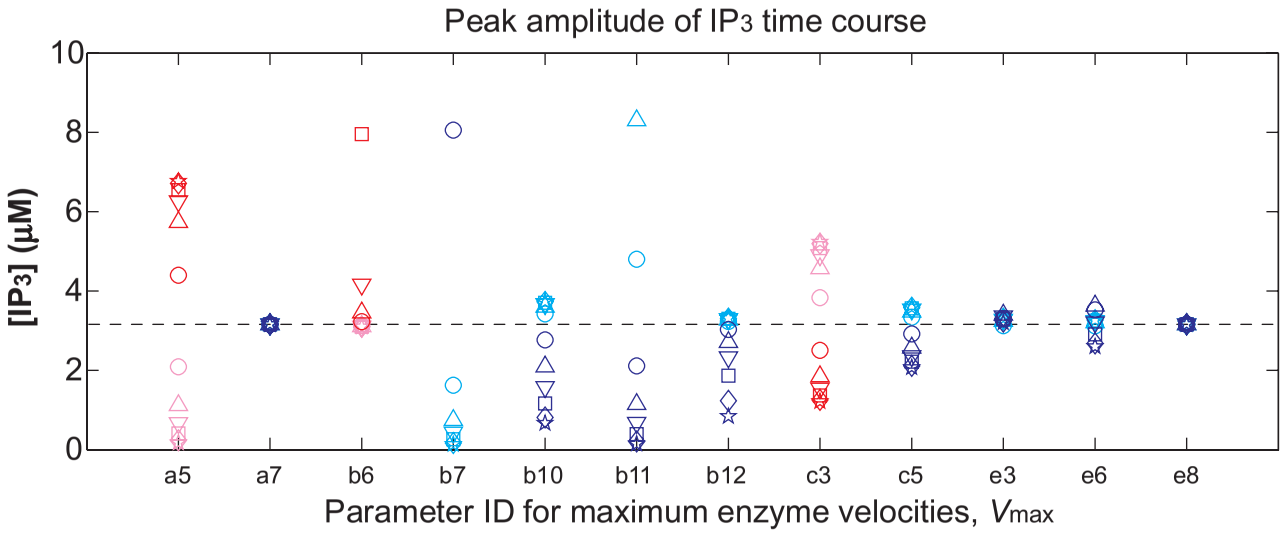

Supplemental Figure 2E

	x1/100	x1/50	x1/20	x1/10	x1/5	x1/2	x2	x5	x10	x20	x50	x100
known	☆	◇	□	▽	△	○	○	△	▽	□	◇	☆
unknown	☆	◇	□	▽	△	○	○	△	▽	□	◇	☆

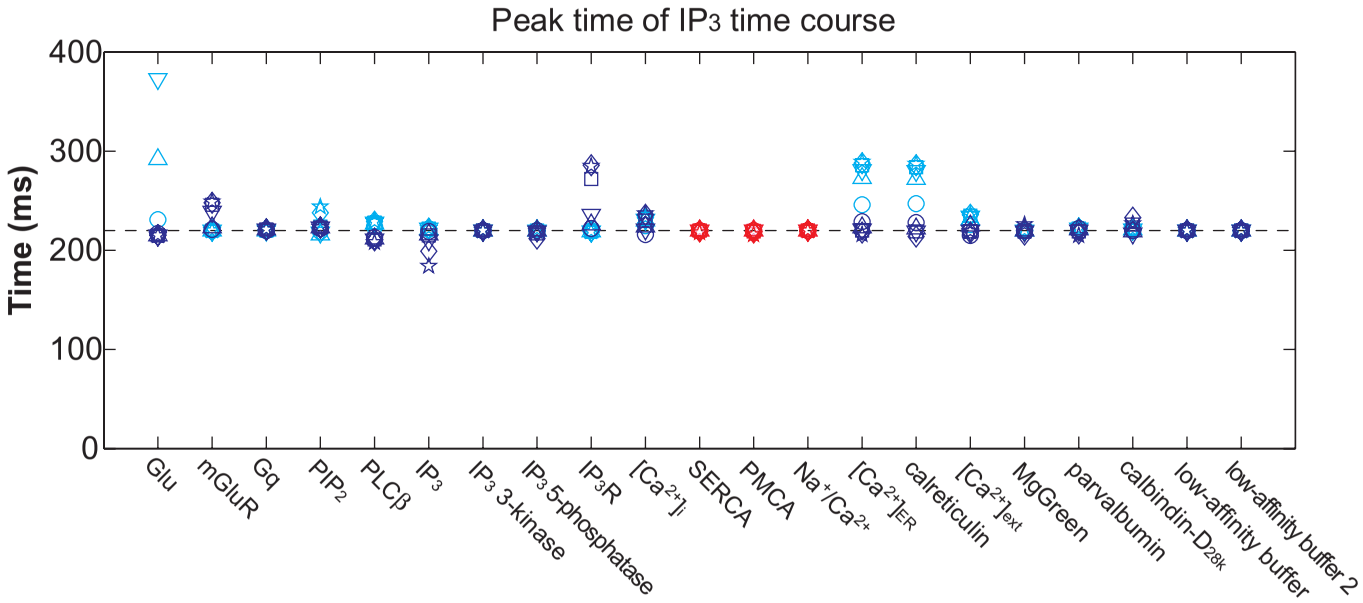

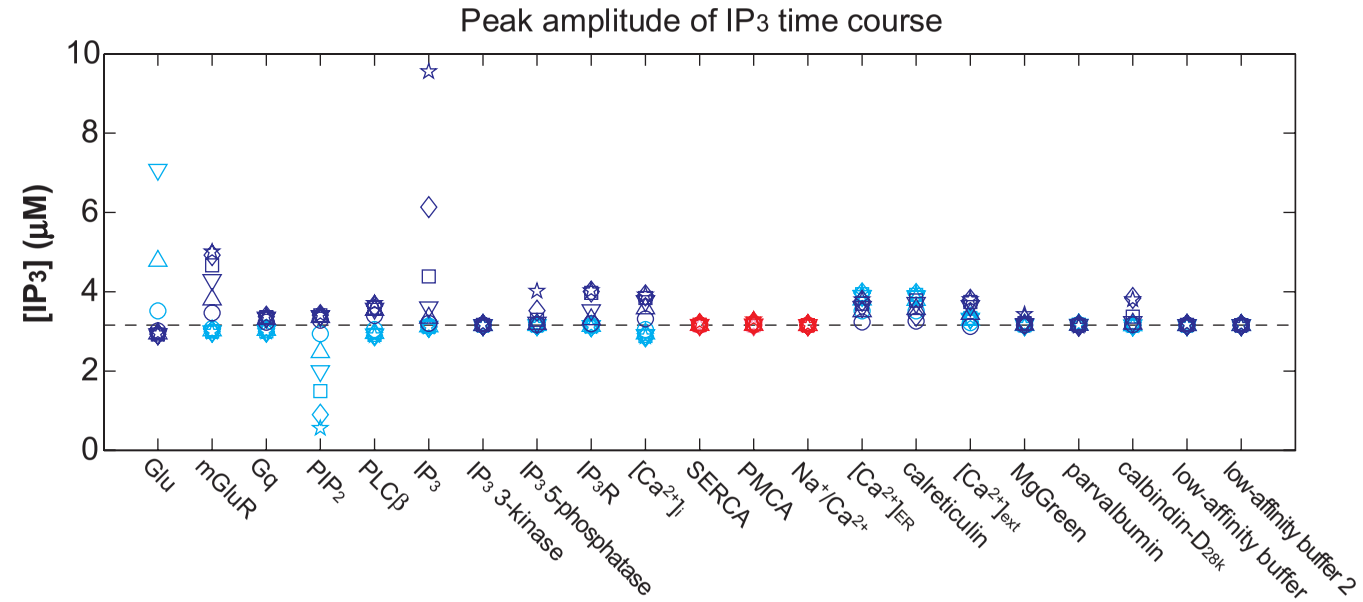

Supplemental Figure 2F

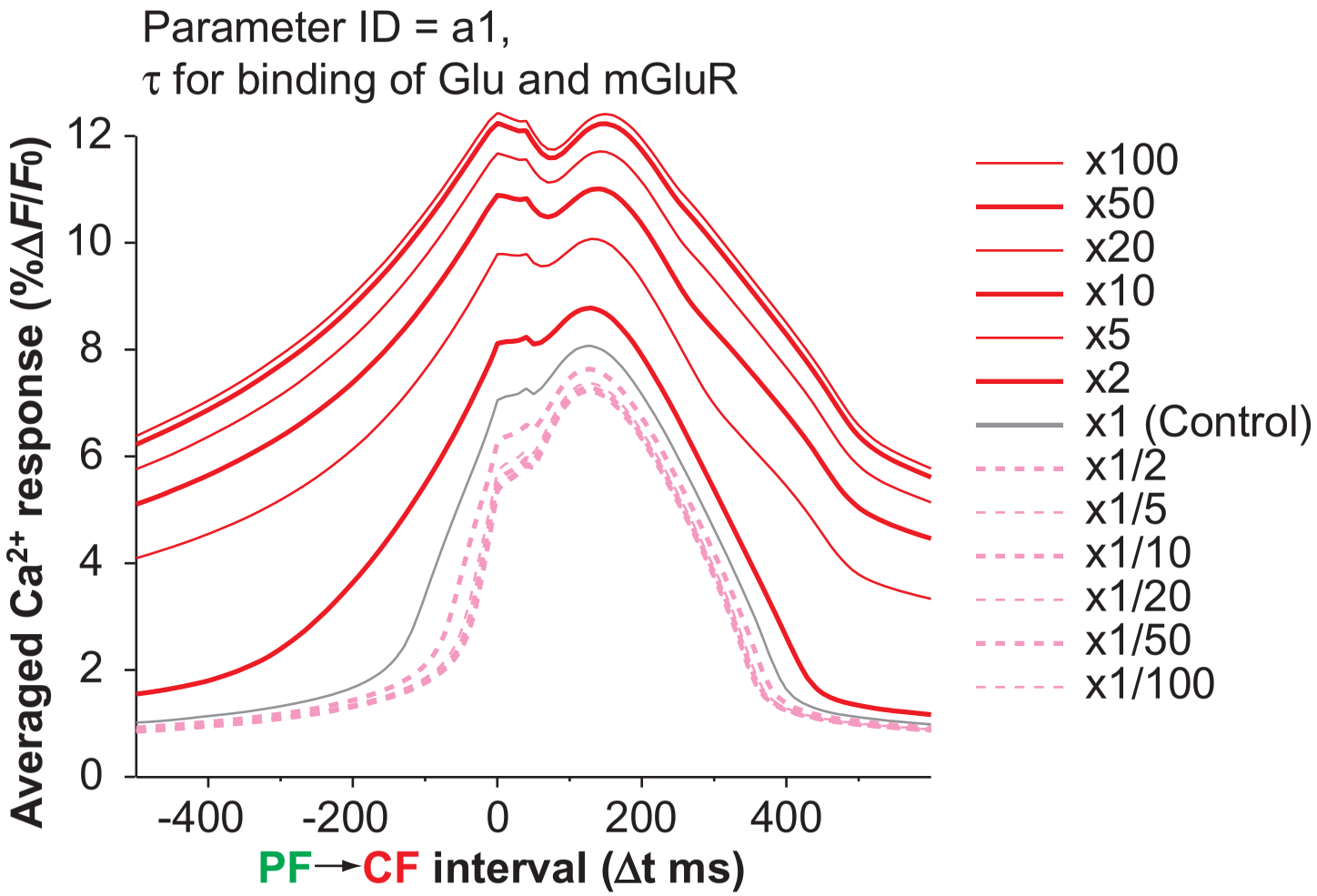

Supplemental Figure 2G

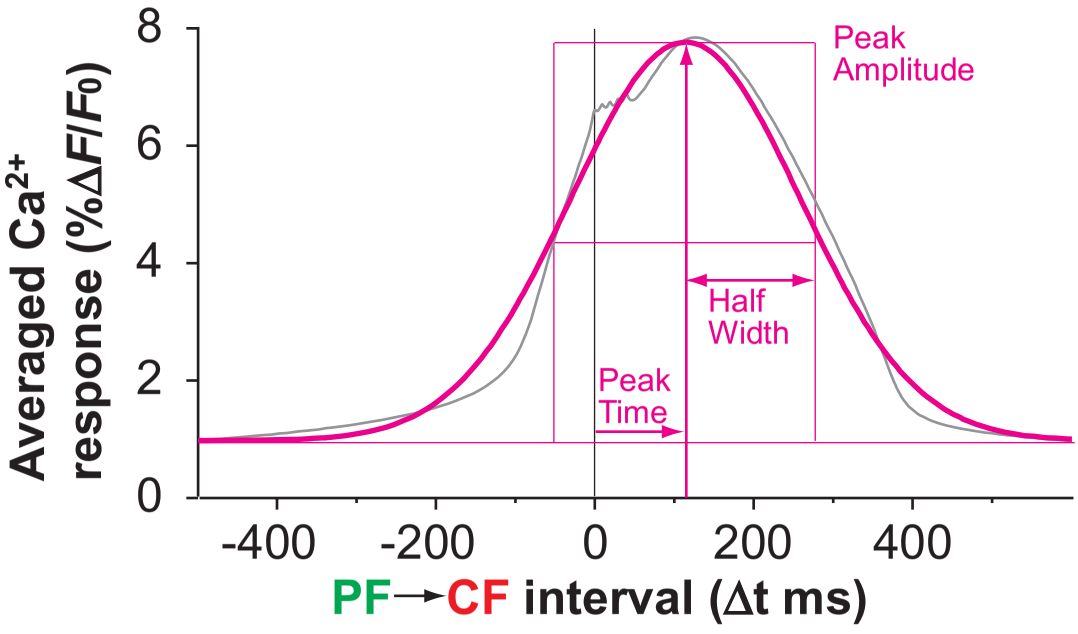

Supplemental Figure 2H

	x1/100	x1/50	x1/20	x1/10	x1/5	x1/2	x2	x5	x10	x20	x50	x100
known	☆	◇	□	▽	△	○	○	△	▽	□	◇	☆
unknown	☆	◇	□	▽	△	○	○	△	▽	□	◇	☆

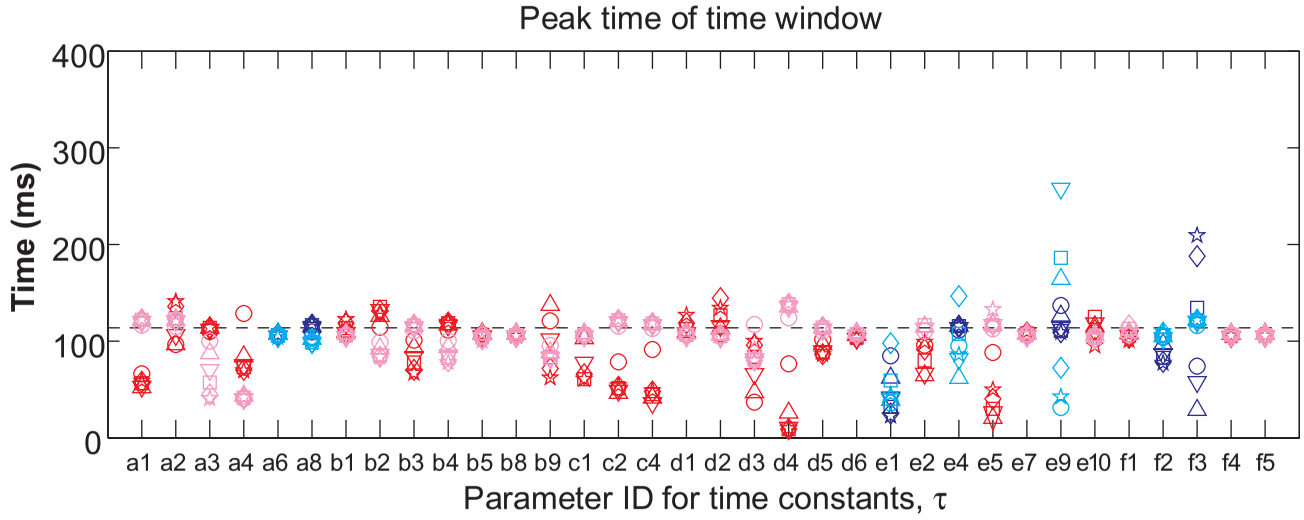

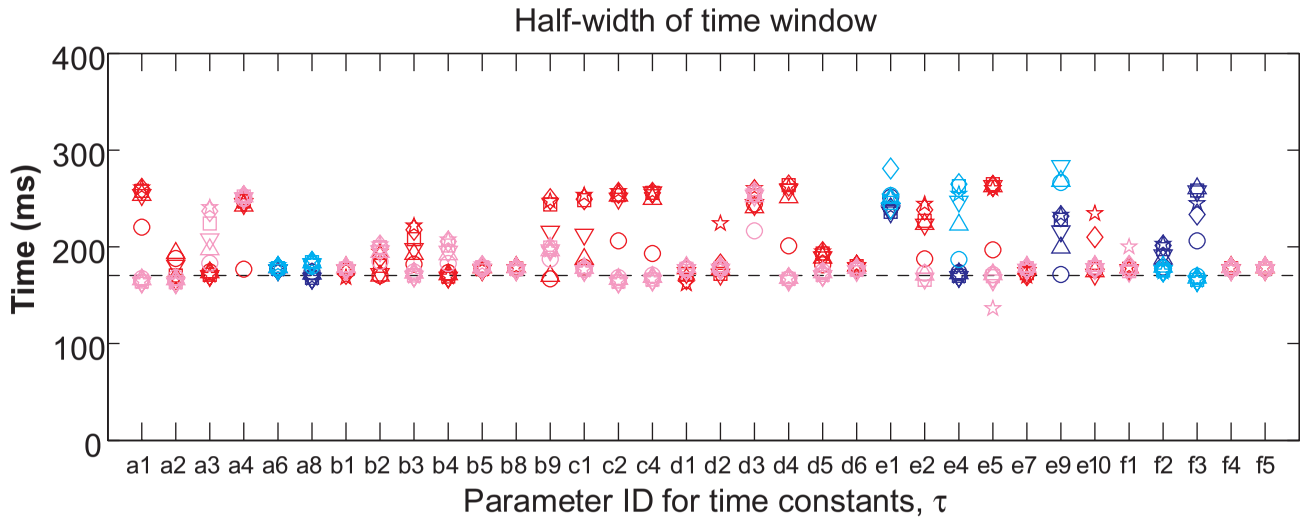

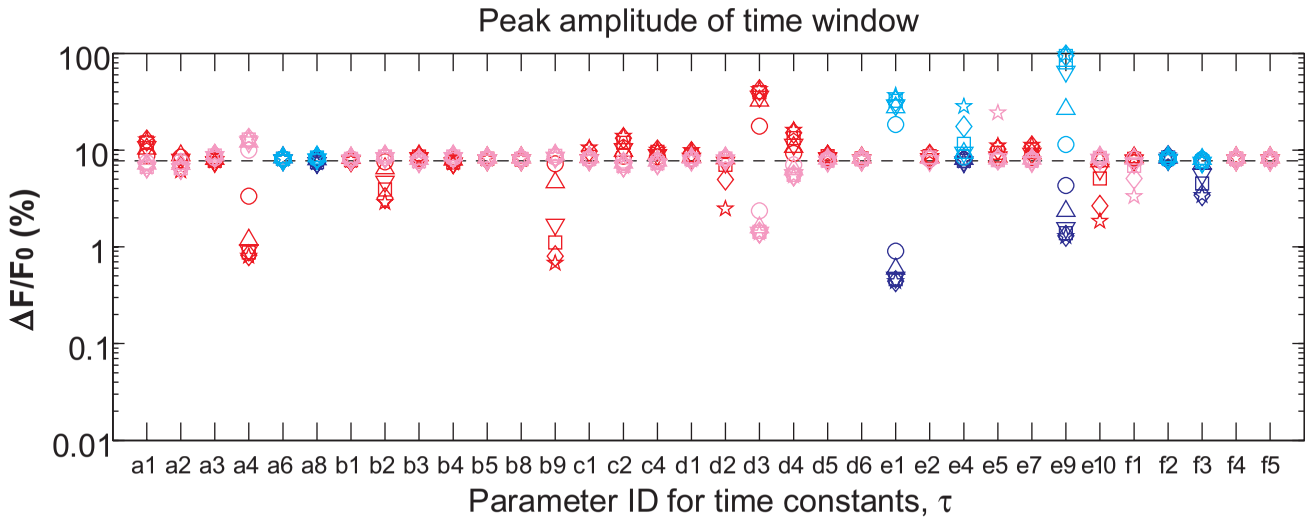

Supplemental Figure 2I

	x1/100	x1/50	x1/20	x1/10	x1/5	x1/2	x2	x5	x10	x20	x50	x100
known	☆	◇	□	▽	△	○	○	△	▽	□	◇	☆
unknown	☆	◇	□	▽	△	○	○	△	▽	□	◇	☆

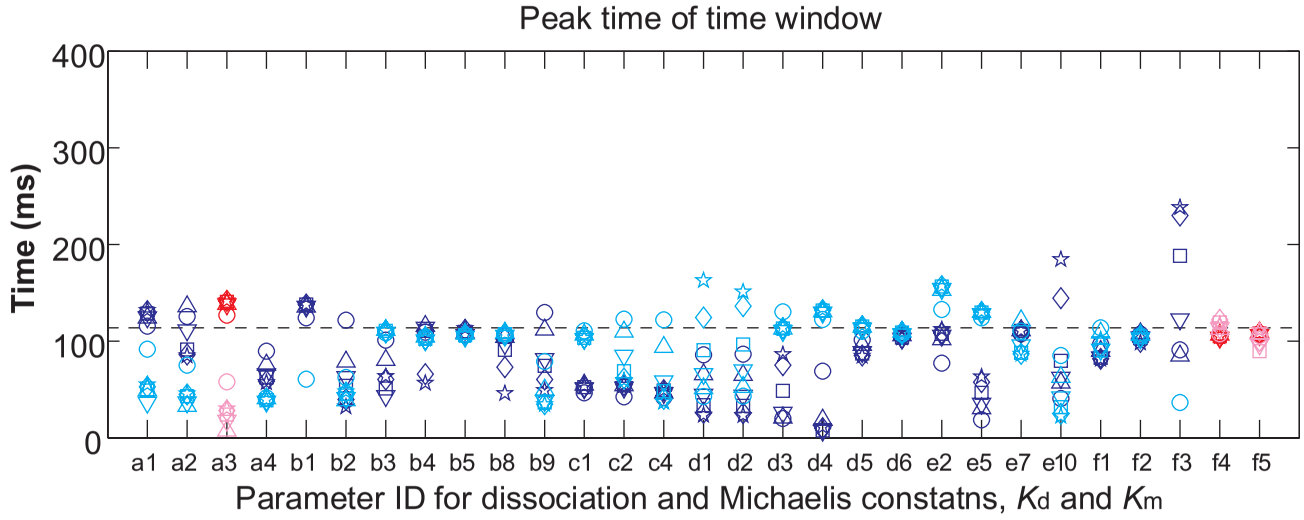

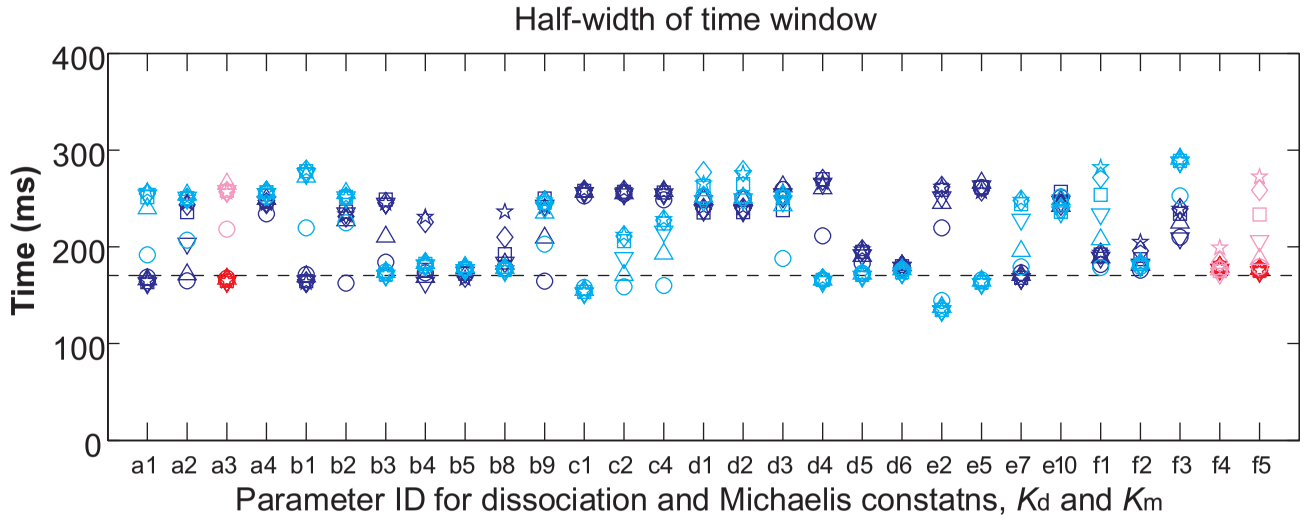

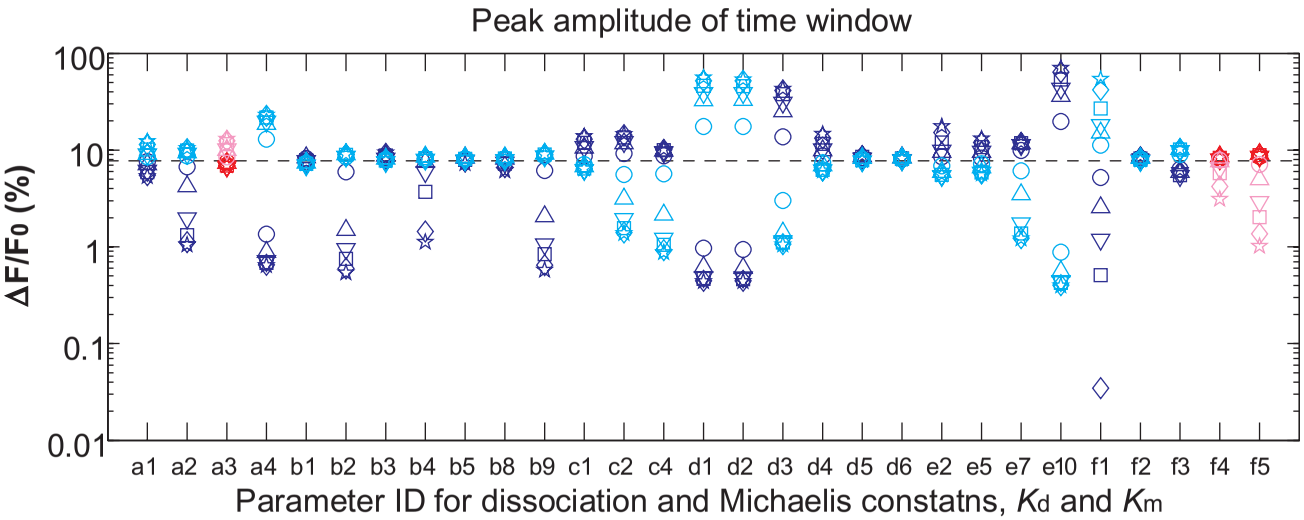

Supplemental Figure 2J

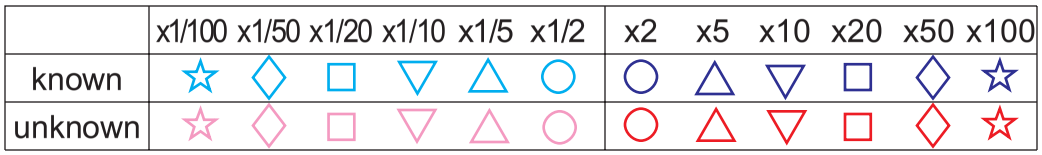

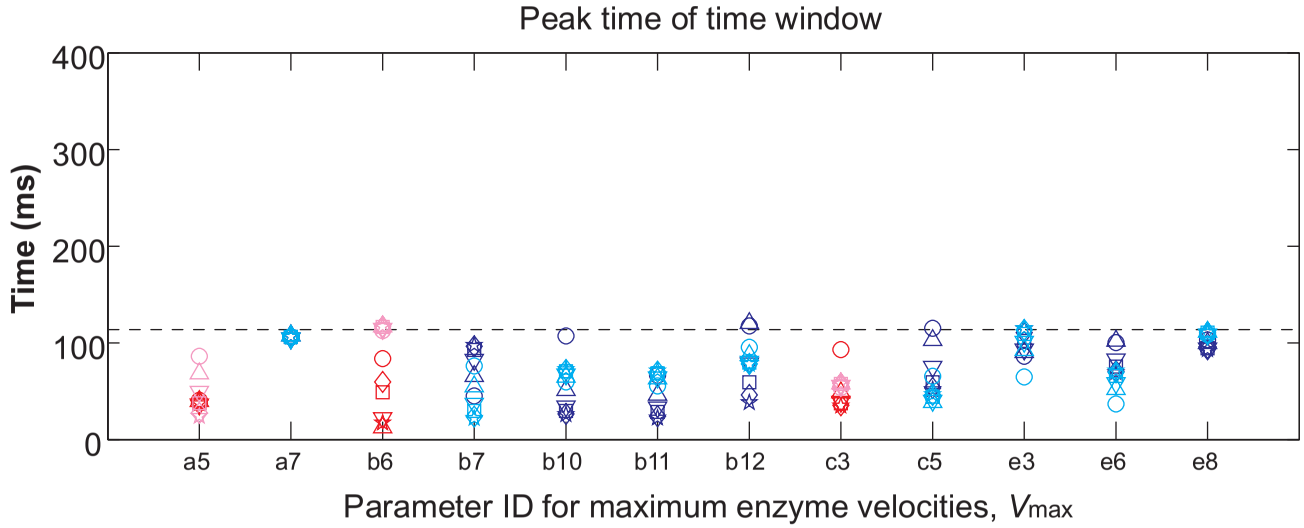

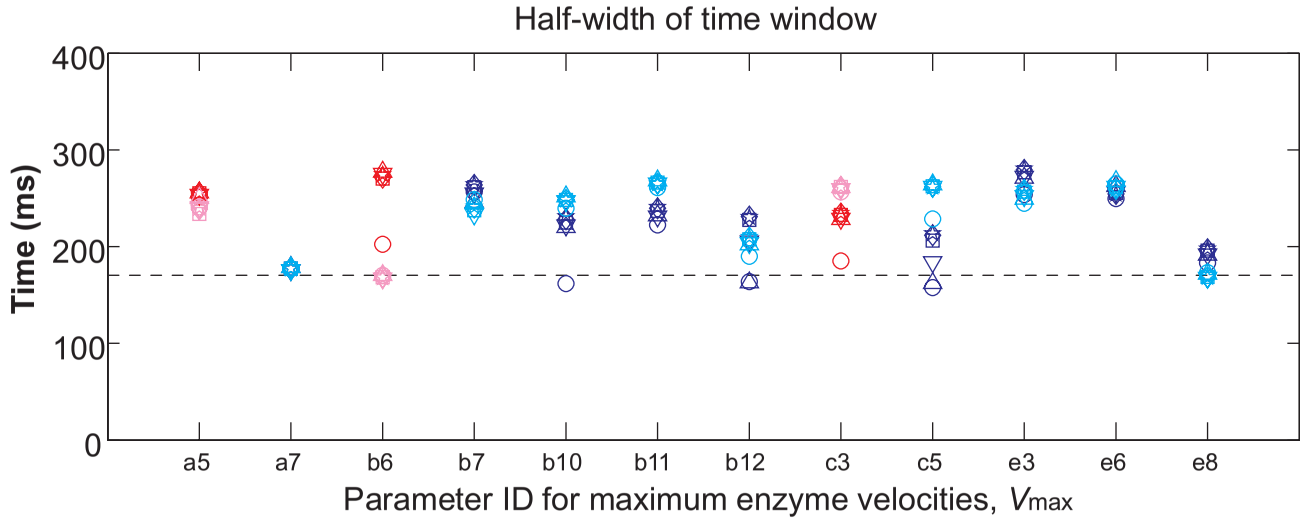

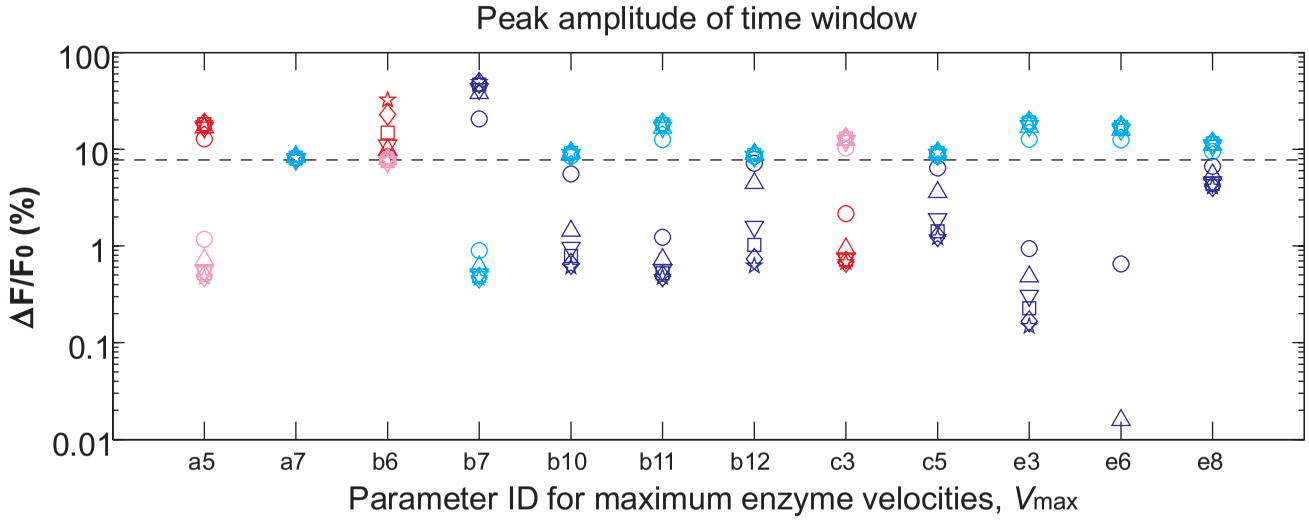

Supplemental Figure 2K

	x1/100	x1/50	x1/20	x1/10	x1/5	x1/2	x2	x5	x10	x20	x50	x100
known	☆	◇	□	▽	△	○	○	△	▽	□	◇	☆
unknown	☆	◇	□	▽	△	○	○	△	▽	□	◇	☆